PERFORMANCE OF A BANDLIMITED TRELLIS DECODING RECEIVER FOR MSK CLASS MODULATIONS IN ADJACENT CHANNEL INTERFERENCE

by

James Harley

A Thesis
Presented to the Faculty of Graduate Studies
in Partial Fulfillment of the Requirements
for the Degree

MASTER OF SCIENCE

Department of Electrical & Computer Engineering
University of Manitoba
Winnipeg, Manitoba

Canada

Name _____

Dissertation Abstracts International and Masters Abstracts International are arranged by broad, general subject categories. Please select the one subject which most nearly describes the content of your dissertation or thesis. Enter the corresponding four-digit code in the spaces provided.

Electronics and Electrical

SUBJECT TERM

`0 5 4 4` **UMI**

SUBJECT CODE

Subject Categories

THE HUMANITIES AND SOCIAL SCIENCES

COMMUNICATIONS AND THE ARTS
Architecture 0729
Art History 0377
Cinema 0900
Dance 0378
Fine Arts 0357
Information Science 0723
Journalism 0391
Library Science 0399
Mass Communications 0708
Music 0413
Speech Communication 0459
Theater 0465

EDUCATION
General 0515
Administration 0514
Adult and Continuing 0516
Agricultural 0517
Art 0273
Bilingual and Multicultural 0282
Business 0688
Community College 0275
Curriculum and Instruction 0727
Early Childhood 0518
Elementary 0524
Finance 0277
Guidance and Counseling 0519
Health 0680
Higher 0745
History of 0520
Home Economics 0278
Industrial 0521
Language and Literature 0279
Mathematics 0280
Music 0522
Philosophy of 0998
Physical 0523

Psychology 0525
Reading 0535
Religious 0527
Sciences 0714
Secondary 0533
Social Sciences 0534
Sociology of 0340
Special 0529
Teacher Training 0530
Technology 0710
Tests and Measurements 0288
Vocational 0747

LANGUAGE, LITERATURE AND LINGUISTICS
Language
  General 0679
  Ancient 0289
  Linguistics 0290
  Modern 0291
Literature
  General 0401
  Classical 0294
  Comparative 0295
  Medieval 0297
  Modern 0298
  African 0316
  American 0591
  Asian 0305
  Canadian (English) 0352
  Canadian (French) 0355
  English 0593
  Germanic 0311
  Latin American 0312
  Middle Eastern 0315
  Romance 0313
  Slavic and East European 0314

PHILOSOPHY, RELIGION AND THEOLOGY
Philosophy 0422
Religion
  General 0318
  Biblical Studies 0321
  Clergy 0319
  History of 0320
  Philosophy of 0322
Theology 0469

SOCIAL SCIENCES
American Studies 0323
Anthropology
  Archaeology 0324
  Cultural 0326
  Physical 0327
Business Administration
  General 0310
  Accounting 0272
  Banking 0770
  Management 0454
  Marketing 0338
Canadian Studies 0385
Economics
  General 0501
  Agricultural 0503
  Commerce-Business 0505
  Finance 0508
  History 0509
  Labor 0510
  Theory 0511
Folklore 0358
Geography 0366
Gerontology 0351
History
  General 0578

Ancient 0579
Medieval 0581
Modern 0582
Black 0328
African 0331
Asia, Australia and Oceania 0332
Canadian 0334
European 0335
Latin American 0336
Middle Eastern 0333
United States 0337
History of Science 0585
Law 0398
Political Science
  General 0615
  International Law and
    Relations 0616
  Public Administration 0617
Recreation 0814
Social Work 0452
Sociology
  General 0626
  Criminology and Penology ... 0627
  Demography 0938
  Ethnic and Racial Studies 0631
  Individual and Family
    Studies 0628
  Industrial and Labor
    Relations 0629
  Public and Social Welfare 0630
  Social Structure and
    Development 0700
  Theory and Methods 0344
Transportation 0709
Urban and Regional Planning 0999
Women's Studies 0453

THE SCIENCES AND ENGINEERING

BIOLOGICAL SCIENCES
Agriculture
  General 0473
  Agronomy 0285
  Animal Culture and
    Nutrition 0475
  Animal Pathology 0476
  Food Science and
    Technology 0359
  Forestry and Wildlife 0478
  Plant Culture 0479
  Plant Pathology 0480
  Plant Physiology 0817
  Range Management 0777
  Wood Technology 0746
Biology
  General 0306
  Anatomy 0287
  Biostatistics 0308
  Botany 0309
  Cell 0379
  Ecology 0329
  Entomology 0353
  Genetics 0369
  Limnology 0793
  Microbiology 0410
  Molecular 0307
  Neuroscience 0317
  Oceanography 0416
  Physiology 0433
  Radiation 0821
  Veterinary Science 0778
  Zoology 0472
Biophysics
  General 0786
  Medical 0760

EARTH SCIENCES
Biogeochemistry 0425
Geochemistry 0996

Geodesy 0370
Geology 0372
Geophysics 0373
Hydrology 0388
Mineralogy 0411
Paleobotany 0345
Paleoecology 0426
Paleontology 0418
Paleozoology 0985
Palynology 0427
Physical Geography 0368
Physical Oceanography 0415

HEALTH AND ENVIRONMENTAL SCIENCES
Environmental Sciences 0768
Health Sciences
  General 0566
  Audiology 0300
  Chemotherapy 0992
  Dentistry 0567
  Education 0350
  Hospital Management 0769
  Human Development 0758
  Immunology 0982
  Medicine and Surgery 0564
  Mental Health 0347
  Nursing 0569
  Nutrition 0570
  Obstetrics and Gynecology .. 0380
  Occupational Health and
    Therapy 0354
  Ophthalmology 0381
  Pathology 0571
  Pharmacology 0419
  Pharmacy 0572
  Physical Therapy 0382
  Public Health 0573
  Radiology 0574
  Recreation 0575

Speech Pathology 0460
Toxicology 0383
Home Economics 0386

PHYSICAL SCIENCES
Pure Sciences
Chemistry
  General 0485
  Agricultural 0749
  Analytical 0486
  Biochemistry 0487
  Inorganic 0488
  Nuclear 0738
  Organic 0490
  Pharmaceutical 0491
  Physical 0494
  Polymer 0495
  Radiation 0754
Mathematics 0405
Physics
  General 0605
  Acoustics 0986
  Astronomy and
    Astrophysics 0606
  Atmospheric Science 0608
  Atomic 0748
  Electronics and Electricity 0607
  Elementary Particles and
    High Energy 0798
  Fluid and Plasma 0759
  Molecular 0609
  Nuclear 0610
  Optics 0752
  Radiation 0756
  Solid State 0611
Statistics 0463

Applied Sciences
Applied Mechanics 0346
Computer Science 0984

Engineering
  General 0537
  Aerospace 0538
  Agricultural 0539
  Automotive 0540
  Biomedical 0541
  Chemical 0542
  Civil 0543
  Electronics and Electrical 0544
  Heat and Thermodynamics ... 0348
  Hydraulic 0545
  Industrial 0546
  Marine 0547
  Materials Science 0794
  Mechanical 0548
  Metallurgy 0743
  Mining 0551
  Nuclear 0552
  Packaging 0549
  Petroleum 0765
  Sanitary and Municipal 0554
  System Science 0790
Geotechnology 0428
Operations Research 0796
Plastics Technology 0795
Textile Technology 0994

PSYCHOLOGY
General 0621
Behavioral 0384
Clinical 0622
Developmental 0620
Experimental 0623
Industrial 0624
Personality 0625
Physiological 0989
Psychobiology 0349
Psychometrics 0632
Social 0451

Nom _____

Dissertation Abstracts International est organisé en catégories de sujets. Veuillez s.v.p. choisir le sujet qui décrit le mieux votre thèse et inscrivez le code numérique approprié dans l'espace réservé ci-dessous.

SUJET

CODE DE SUJET

☐☐☐☐☐ U·M·I

Catégories par sujets

HUMANITÉS ET SCIENCES SOCIALES

COMMUNICATIONS ET LES ARTS
Architecture	0729
Beaux-arts	0357
Bibliothéconomie	0399
Cinéma	0900
Communication verbale	0459
Communications	0708
Danse	0378
Histoire de l'art	0377
Journalisme	0391
Musique	0413
Sciences de l'information	0723
Théâtre	0465

ÉDUCATION
Généralités	515
Administration	0514
Art	0273
Collèges communautaires	0275
Commerce	0688
Économie domestique	0278
Éducation permanente	0516
Éducation préscolaire	0518
Éducation sanitaire	0680
Enseignement agricole	0517
Enseignement bilingue et multiculturel	0282
Enseignement industriel	0521
Enseignement primaire.	0524
Enseignement professionnel	0747
Enseignement religieux	0527
Enseignement secondaire	0533
Enseignement spécial	0529
Enseignement supérieur	0745
Évaluation	0288
Finances	0277
Formation des enseignants	0530
Histoire de l'éducation	0520
Langues et littérature	0279

Lecture	0535
Mathématiques	0280
Musique	0522
Orientation et consultation	0519
Philosophie de l'éducation	0998
Physique	0523
Programmes d'études et enseignement	0727
Psychologie	0525
Sciences	0714
Sciences sociales	0534
Sociologie de l'éducation	0340
Technologie	0710

LANGUE, LITTÉRATURE ET LINGUISTIQUE
Langues
Généralités	0679
Anciennes	0289
Linguistique	0290
Modernes	0291

Littérature
Généralités	0401
Anciennes	0294
Comparée	0295
Mediévale	0297
Moderne	0298
Africaine	0316
Américaine	0591
Anglaise	0593
Asiatique	0305
Canadienne (Anglaise)	0352
Canadienne (Française)	0355
Germanique	0311
Latino-américaine	0312
Moyen-orientale	0315
Romane	0313
Slave et est-européenne	0314

PHILOSOPHIE, RELIGION ET THÉOLOGIE
Philosophie	0422

Religion
Généralités	0318
Clergé	0319
Études bibliques	0321
Histoire des religions	0320
Philosophie de la religion	0322
Théologie	0469

SCIENCES SOCIALES
Anthropologie
Archéologie	0324
Culturelle	0326
Physique	0327
Droit	0398

Économie
Généralités	0501
Commerce-Affaires	0505
Économie agricole	0503
Economie du travail	0510
Finances	0508
Histoire	0509
Théorie	0511
Études américaines	0323
Études canadiennes	0385
Études féministes	0453
Folklore	0358
Géographie	0366
Gérontologie	0351

Gestion des affaires
Généralités	0310
Administration	0454
Banques	0770
Comptabilité	0272
Marketing	0338

Histoire
Histoire générale	0578

Ancienne	0579
Médiévale	0581
Moderne	0582
Histoire des noirs	0328
Africaine	0331
Canadienne	0334
États-Unis	0337
Européenne	0335
Moyen-orientale	0333
Latino-américaine	0336
Asie, Australie et Océanie	0332
Histoire des sciences	0585
Loisirs	0814
Planification urbaine et régionale	0999

Science politique
Généralités	0615
Administration publique	0617
Droit et relations internationales	0616

Sociologie
Généralités	0626
Aide et bien-être social	0630
Criminologie et établissements pénitentiaires	0627
Démographie	0938
Études de l'individu et de la famille	0628
Études des relations interethniques et des relations raciales	0631
Structure et développement social	0700
Théorie et méthodes.	0344
Travail et relations industrielles	0629
Transports	0709
Travail social	0452

SCIENCES ET INGÉNIERIE

SCIENCES BIOLOGIQUES
Agriculture
Généralités	0473
Agronomie.	0285
Alimentation et technologie alimentaire	0359
Culture	0479
Élevage et alimentation	0475
Exploitation des péturages	0777
Pathologie animale	0476
Pathologie végétale	0480
Physiologie végétale	0817
Sylviculture et faune	0478
Technologie du bois	0746

Biologie
Généralités	0306
Anatomie	0287
Biologie (Statistiques)	0308
Biologie moléculaire	0307
Botanique	0309
Cellule	0379
Écologie	0329
Entomologie	0353
Génétique	0369
Limnologie	0793
Microbiologie	0410
Neurologie	0317
Océanographie	0416
Physiologie	0433
Radiation	0821
Science vétérinaire	0778
Zoologie	0472

Biophysique
Généralités	0786
Medicale	0760

SCIENCES DE LA TERRE
Biogéochimie	0425
Géochimie	0996
Géodésie	0370
Géographie physique	0368

Géologie	0372
Géophysique	0373
Hydrologie	0388
Minéralogie	0411
Océanographie physique	0415
Paléobotanique	0345
Paléoécologie	0426
Paléontologie	0418
Paléozoologie	0985
Palynologie	0427

SCIENCES DE LA SANTÉ ET DE L'ENVIRONNEMENT
Économie domestique	0386
Sciences de l'environnement	0768

Sciences de la santé
Généralités	0566
Administration des hipitaux	0769
Alimentation et nutrition	0570
Audiologie	0300
Chimiothérapie	0992
Dentisterie	0567
Développement humain	0758
Enseignement	0350
Immunologie	0982
Loisirs	0575
Médecine du travail et thérapie	0354
Médecine et chirurgie	0564
Obstétrique et gynécologie	0380
Ophtalmologie	0381
Orthophonie	0460
Pathologie	0571
Pharmacie	0572
Pharmacologie	0419
Physiothérapie	0382
Radiologie	0574
Santé mentale	0347
Santé publique	0573
Soins infirmiers	0569
Toxicologie	0383

SCIENCES PHYSIQUES
Sciences Pures
Chimie
Généralités	0485
Biochimie	487
Chimie agricole	0749
Chimie analytique	0486
Chimie minérale	0488
Chimie nucléaire	0738
Chimie organique	0490
Chimie pharmaceutique	0491
Physique	0494
PolymÇres	0495
Radiation	0754
Mathématiques	0405

Physique
Généralités	0605
Acoustique	0986
Astronomie et astrophysique	0606
Electronique et électricité	0607
Fluides et plasma	0759
Météorologie	0608
Optique	0752
Particules (Physique nucléaire)	0798
Physique atomique	0748
Physique de l'état solide	0611
Physique moléculaire	0609
Physique nucléaire	0610
Radiation	0756
Statistiques	0463

Sciences Appliqués Et Technologie
Informatique	0984

Ingénierie
Généralités	0537
Agricole	0539
Automobile	0540

Biomédicale	0541
Chaleur et ther modynamique	0348
Conditionnement (Emballage)	0549
Génie aérospatial	0538
Génie chimique	0542
Génie civil	0543
Génie électronique et électrique	0544
Génie industriel	0546
Génie mécanique	0548
Génie nucléaire	0552
Ingénierie des systèmes	0790
Mécanique navale	0547
Métallurgie	0743
Science des matériaux	0794
Technique du pétrole	0765
Technique minière	0551
Techniques sanitaires et municipales	0554
Technologie hydraulique	0545
Mécanique appliquée	0346
Géotechnologie	0428
Matières plastiques (Technologie)	0795
Recherche opérationnelle	0796
Textiles et tissus (Technologie)	0794

PSYCHOLOGIE
Généralités	0621
Personnalité	0625
Psychobiologie	0349
Psychologie clinique	0622
Psychologie du comportement	0384
Psychologie du développement	0620
Psychologie expérimentale	0623
Psychologie industrielle	0624
Psychologie physiologique	0989
Psychologie sociale	0451
Psychométrie	0632

PERFORMANCE OF A BANDLIMITED TRELLIS DECODING

RECEIVER FOR MSK CLASS MODULATIONS IN ADJACENT

CHANNEL INTERFERENCE

BY

JAMES HARLEY

A Thesis submitted to the Faculty of Graduate Studies of the University of Manitoba
in partial fulfillment of the requirements of the degree of

MASTER OF SCIENCE

© 1996

ACKNOWLEDGMENTS

ABSTRACT

The performance of a bandlimited trellis decoding receiver (BTR) is investigated for MSK class modulations in adjacent channel interference (ACI). The receiver consists of a front-end bandlimiting filter, a Nyquist sampler, and Viterbi Algorithm decoding of the trellis matched to the sampled truncated impulse response of the channel. As there is no known optimum detector in non-Gaussian ACI, this receiver is a candidate for superior performance in ACI compared to the matched filter (MF) receiver. Analysis as well as simulation results show that the BTR has indistinguishable performance compared to the optimum MF in additive white Gaussian noise only for Offset Quadrature Phase Shift Keying (OQPSK), Sinusoidal Frequency Shift Keying (SFSK) and Minimum Shift Keying (MSK). In ACI the BTR demonstrates considerable more robustness than the MF, suppressing up to 4.8 dB more ACI.

I hereby declare that I am the sole author of this thesis.

I authorize the University of Manitoba to lend this thesis to other institutions or individuals for the purpose of scholarly research.

James Harley.

I further authorize the University of Manitoba to reproduce this thesis by photocopying or by other means, in total or in part, at the request of other institutions or individuals for the purpose of scholarly research.

James Harley

TABLE OF CONTENTS

LIST OF FIGURES

LIST OF TABLES

1. INTRODUCTION

In the ever crowded radio spectrum which demands closer spectral packing of signals, adjacent channel interference has become a serious limiting factor in Frequency Division Multiple Access (FDMA) systems. Furthermore high levels of adjacent channel interference (ACI) can be experienced with the near-far problem , where a user receives a far distance signal in the proximity of someone else's transmission. For FDMA systems, the constant envelope minimum shift keying (MSK) type modulations is an attractive choice. The constant envelope constraint allows the use of less expensive, more power efficient nonlinear amplifiers in the transmission. Although the constant envelope implies a wider bandwidth compared to ideal Nyquist pulses, these constant envelope modulations still have attractive bandwidth properties with modulations such as MSK and Gaussian minimum shift keying (GMSK) .

A lot of the previous work in ACI suppression investigated the modulation question, culminating in the optimization of the baseband waveform to minimize the fraction of out of band power for a particular bandwidth [1] . Only recently has there been work on receiver design for improved performance in ACI compared to the standard quadrature correlation receiver (MF). This work [2]-[3] used wide front end filtering while sampling at twice the receiver's bandwidth in conjunction with either linear equalizer or decision feedback equalizers. For the case of one antenna with a signal in intersymbol interference (ISI) and ACI , this receiver showed some improvements in ACI suppression.

This thesis investigates the design and performance of a receiver for ACI suppression and additive white Gaussian noise (AWGN) mitigation. The approach taken is to strictly bandlimit the received signal and sample at the Nyquist rate to provide sufficient statistics of the bandlimited signal for a trellis decoder. The trellis decoder is matched to the truncated bandlimited signal and proceeds with a sub optimum maximum

likelihood sequence estimation in the presence of AWGN and the filtered ACI. The receiver, called the bandlimiting trellis decoding receiver (BTR), rejects considerable ACI through narrow bandlimiting filtering and uses the ISI in the trellis decoding for detection. As there is no known optimum detector for non Gaussian ACI in AWGN, the BTR is a candidate for superior performance compared to the traditional matched filter (MF).

1.1 Scope of Thesis

The focus of this thesis is to investigate the performance of the BTR for MSK type modulations in AWGN and ACI. The performance of the BTR is benchmarked with the performance of the MF receiver, which is optimum in AWGN only. The thesis is composed as follows. Chapter two provides a review of classical detection theory for linear signals in AWGN and shows its limitations in the detection of signals in non Gaussian ACI. In addition, this chapter examines three sub-optimum approaches to this signal detection problem; the nuisance parameter approach, joint maximum likelihood sequence estimation (JMLSE), and subspace projection. The BTR is an example of subspace projection, where the received signal is projected onto a bandlimited subspace. Chapter three introduces the MSK type modulations as an example of linear offset quadrature modulation. This chapter then presents the BTR receiver for MSK type modulations, discussing in detail the bandlimiting filter and the resulting intersymbol interference of the signal of interest (SOI) and the statistics of the filtered ACI, as well as the metrics for the trellis decoder in AWGN and in ACI. The first section of Chapter four contains analysis and Monte Carlo simulation results for the performance of the BTR in AWGN compared to the optimum performance of the MF. The last section presents extensive Monte Carlo simulations for the performance of the BTR compared to the MF in AWGN and ACI, as well as a simplified analysis of the BTR based on modeling the

filtered ACI as white Gaussian noise. The final chapter summarizes the results of the thesis and indicates further areas of study.

2. LITERATURE REVIEW

This chapter first provides a review of classical detection theory in AWGN for linear signals (maximum likelihood detection) and then shows its limitations in the detection of signals in non Gaussian ACI. The review goes into some detail because establishing the vector space concepts is important in understanding the rest of the chapter. It also serves as background for the BTR, which performs MLSE on a bandlimited subspace. Three standard sub-optimum approaches, the nuisance parameter approach, joint maximum likelihood sequence estimation (JMLSE), and subspace projection are examined in the context of this signal detection problem. The nuisance parameter approach is shown to be untractable as a realizable receiver, while the JMLSE results in excessive hardware complexity. Both the fractionally spaced DFE and the BTR are discussed as examples of the subspace projection approach.

2.1 Classical Detection in AWGN.

The discussion focuses on the case of detecting linear signals in AWGN. For MSK class modulation, the transmitted signal can be considered as two linear antipodal signals in quadrature. Consider symbol by symbol detection, where the received signal for binary signaling is:

$$r(t) = s_i(t) + n(t) \quad 0 \le t \le T \quad i=1,2 \tag{2.1}$$

where either hypothesis $s_1(t)$ or $s_2(t)$ is equally likely, and $n(t)$ is white Gaussian noise with spectral density No/2 watts/Hz. The maximum a posterior (MAP) decision rule, given $r(t)$, is to choose the hypothesis which is most likely, in other words, choose the hypothesis whose a posterior density function $f\{s_i(t) \mid r(t)\}$ has the largest value. When

the hypotheses are equally likely, this decision rule can be restated in terms of $f\{r(t) \mid s_i(t)\}$ when considering the Bayes rule, since:

$$f\{ s_i(t) \mid r(t) \} = \frac{f\{ r(t) \mid s_i(t)\}P\{s_i(t)\}}{f\{r(t)\}} \tag{2.2}$$

Both $P\{s_i(t)\}$ (the probability of hypothesis of si(t)) and $f\{r(t)\}$ have the same value for either hypothesis, hence choosing the hypothesis with largest $f\{r(t) \mid s_i(t)\}$, which is known as the maximum likelihood rule (ML), is equivalent to the MAP rule. In the continuous signal case, the density function $f\{r(t) \mid s_i(t)\}$ is clearly not well formulated. Following the Karhunen-Loeve approach, this density function can be well defined by converting the continuous signal r(t) into a set of discrete values, called sufficient statistics [4].

The Karhunen-Loeve approach is to project r(t) onto an arbitrary set of orthonormal functions $\{\varphi_1(t),\ \varphi_2(t),...\ \}$ which span $L^2(T)$, under the constraint that the set of random variables $\{r_j\ \}$, where $r_j = \int_0^T r(t)\varphi_j(t)dt$, are uncorrelated with each other. Since the noise has Gaussian statistics, then each r_j is Gaussian because the output of any linear operation (here integration) on a Gaussian process is Gaussian as well. Note that the Gaussian noise in this case is white, therefore any arbitrary set of orthonormal functions satisfy the Karhunen-Loeve condition. Hence the set of $\{r_j\}$ are independent Gaussian random variables with mean $s_{i,j} = \int_0^T s_i(t)\varphi_j(t)dt$ and variance No/2 watts. As the original signal r(t) can be reconstructed from $\{r_j\ \}$, the decision rule can be equivalently applied to $\{r_j\ \}$. Since the $f\{\ r \mid s_i\ \}$ are Gaussian densities, the decision rule can be more compactly implemented by taking the natural log of the ratio of these two densities and comparing the result to a threshold. This test is called the log likelihood test $\Lambda(r)$ and is defined here as:

$$\Lambda(r) = \ln[\ f\{r \mid s_1\}/\ f\{r \mid s_2\}\ ]$$

if $\Lambda(r) > 0$ choose $s_1(t)$ as the transmitted signal

if $\Lambda(r) < 0$ choose $s_2(t)$ as the transmitted signal $\tag{2.3}$

6

$$\Lambda(\mathbf{r}) = \frac{1}{No} \left[-\sum_{j=1}^{\infty} (r_j - s_{1,j})^2 + \sum_{j=1}^{\infty} (r_j - s_{2,j})^2 \right]$$

where $r_j = \int_0^T r(t)\varphi_j(t)dt$ and $s_{i,j} = \int_0^T s_i(t)\varphi_j(t)dt$.

Note that the arbitrary set of orthonormal functions in the case of AWGN can be chosen to minimize the number of dimensions to evaluate $\Lambda(\mathbf{r})$. For a signal set of two signals, up to two orthornormal basis signals can represent either two signals exactly as a linear combination of these basis signals. The two basis signals can be constructed from the original signal set according to the well known Gram-Schmidt procedure. The complete set of orthornormal signals is now the vector space of the direct sum of the two basis signals and its orthogonal complement. $\Lambda(\mathbf{r})$ can be evaluated up to these two basis dimensions, because the remaining dimensions are orthogonal to $s_1(t)$ and $s_2(t)$ and contribute zero in the inner product terms in $\Lambda(\mathbf{r})$.

An alternative way to evaluate $\Lambda(\mathbf{r})$ is to recognize that as $\{r_j, s_{i,j}\}$ are coefficients of an orthonormal set of functions. According to Parseval's theorem, the right-hand side can be equivalently computed by:

$$\Lambda(\mathbf{r}) = \frac{1}{No} \left[\int_0^T (r(t) - s_1(t))^2 dt - \int_0^T (r(t) - s_2(t))^2 dt \right] \qquad (2.4)$$

Equation (2.4) indicates that the receiver chooses the signal closest to the received signal in Euclidean space. Here the Euclidean space is defined as the set of finite energy complex signals over the (0,T) interval, where the inner product and norm are defined by:

$$\langle x(t), y(t) \rangle = \int_0^T x(t)\overline{y(t)}dt$$

$$\|x(t)\|^2 = \int_0^T |x(t)|^2 dt \qquad (2.5)$$

where $\bar{z}$ denotes the complex conjugate of z. The log likelihood function can be simplified to:

$$\Lambda(\mathbf{r}) = \frac{1}{No}\left[-2\int_0^T r(t)s_1(t)dt + 2\int_0^T r(t)s_2(t)dt + E_1 - E_2\right] \qquad (2.6)$$

where $E_i = \int_0^T s_i^2(t)dt$ joules, for i=1,2, is the energy of $s_i(t)$.

Assuming the receiver knows the energy of the two signals (E_1 and E_2), then the receiver requires only to perform two correlations with the received signal by using two filters with impulse responses $h_i(t)=s_i(T-t)$. These filters are "matched" to the signals $s_1(t)$ and $s_2(t)$ [4].

In the case of a sequence of statistically independent symbols, this maximum likelihood approach can be easily extended to maximum likelihood sequence estimation (MLSE). For binary antipodal signaling, then the received signal is:

$$r(t) = \sum_{j=1}^N a_j p(t-jT) + n(t) \qquad (2.7)$$

where p(t) is an arbitrary waveform defined over (0,T) outside of which it is zero, and a_j are equally likely (1 or -1) independent random variables. The approach here is to determine the most likely sequence of N symbols (or equivalently the 1xN vector $\mathbf{a}$) given r(t). Hence MLSE means choosing $\mathbf{a}$ that has largest $\ln[f\{\mathbf{r} \mid \mathbf{a}\}]$ since each sequence is equally likely . According to the approach outlined above , then

$$\Lambda(\mathbf{r}) = \frac{1}{No}\int_0^{NT}\left(r(t) - \sum_{j=1}^N a_j p(t-jT)\right)^2 dt = \frac{1}{No}\sum_{j=1}^N \int_{(j-1)T}^{jT}\left(r(t) - a_j p(t-jT)\right)^2 dt \qquad (2.8)$$

The vector space concepts are now naturally extended to (0, NT) space. Thus the MLSE receiver chooses the signal sequence closest to the received signal over 0 to NT. Notice that in this case because each symbol is statistically independent from each other and there

is no time overlap between symbols, the MLSE collapses down to symbol by symbol decisions.

2.2 Detection in AWGN and ACI

It is still an open question to find a method to generate a set of orthonormal functions such that the resulting $f \{ \mathbf{r} | \mathbf{a} \}$ in AWGN and ACI leads to a realizable receiver structure. The Karhunen-Loeve expansion method fails in the presence of ACI and AWGN, because of the non-Gaussian statistics of the ACI. Assuming the ACI is wide sense stationary, then even if a set of orthonormal functions are found that satisfy the Karhunen-Loeve condition, it does not follow that the uncorrelated projections on each of these orthornormal functions are statistically independent. Although the joint density function $f \{ \mathbf{r} | \mathbf{a} \}$ could be determined in theory, there is no guarantee that the resulting $f\{ \mathbf{r} | \mathbf{a} \}$ is implementable. Just as the Karhunen-Loeve method is specialized for the additive Gaussian noise case, it is possible that there are specialized methods that apply to certain types of ACI, but up to this date no research has been conducted along these lines.

In general, for the optimum detection of signals in ACI and AWGN, the interpretation of choosing the signal closest to the received signal in Euclidean space has to be abandoned. There is the important case when the ACI is designed to be orthogonal to the space spanned by the signal set of interest (SOI). If the received waveform in this case is projected onto a vector space which is spanned by the SOI then the resulting sufficient statistics have no component due to ACI. The detection problem reduces to the case of detecting the SOI in AWGN. Hence in this case the vector space interpretation can be kept.

Many modulation schemes have been designed to meet this requirement of orthogonality. There are two main obstacles to achieving orthogonality, phase offset and symbol time offset between the SOI and the adjacent channels. Phase offset is the relative

phase difference between carriers, and symbol time offset is the difference in time that a symbol is asserted. The simplest case is when the channels are phase offset but symbol time synchronized. Examples of this case are Frequency Division Multiple Access (FDMA) and Code Division Multiple Access (CDMA). A synchronized FDMA system divides up its frequency band into equal sized bands which are spaced such that non-coherent orthogonality is obtained. Typically FDMA systems use quadrature phase shift keying (QPSK) which requires a 1/T frequency spacing. A synchronized CDMA system on the other hand shares its frequency band with all channels, and ensures orthogonality by supplying each user with an orthogonal spreading code (i.e, orthogonal to all the other codes).

The requirement to be orthogonal for all symbol time offsets say between x(t) (the SOI) and a(t) (the ACI) is harder to achieve. In effect, this means the cross correlation between x(t) and a(t) is zero for all time shifts. In other words,

$$\int_{-\infty}^{\infty} x(t)a(t+\tau)dt = 0 \qquad \text{for all } \tau \qquad (2.9)$$

This cross correlation is simply the convolution of x(t) with a(-t). This condition translated to the frequency domain means that the product $X(f)\overline{A}(f)$ equals zero for all frequencies, where X(f) and A(f) are the Fourier transforms of x(t) and a(t) respectively. Therefore X(f) and A(f) have to be frequency limited in a complementary manner to achieve this condition. One method is for X(f) and A(f) to be bandlimited and sufficiently frequency separated so there is no frequency overlap. Hence, the traditional notion of adjacent bandlimited channels comes naturally out of this discussion. Note that frequency limitation implies an infinite time span for each symbol signal which adds the complication of detecting a sequence of symbols which overlap with each other. One solution to this classic problem of detecting a sequence of bandlimited signals without intersymbol interference is the set of Nyquist pulses .

There are number of situations where non-orthogonal ACI is unavoidable. Constant amplitude modulations like MSK are desired when using amplifiers in the more power efficient non-linear region, or the channel distortion is such, as in fast fading mobile channels, that the orthogonality is destroyed resulting in ACI. There are at least three sub optimum approaches for the receiver design in the presence of unwanted ACI. These are the nuisance parameter, joint estimation, and projection into subspace approaches, each of which are discussed briefly.

2.3 Nuisance Parameter

The nuisance parameter approach has been successfully applied to unwanted random parameters in the SOI itself such as phase uncertainty or amplitude variation due to flat fading channels [5]. It has been suggested that this approach could be applied to ACI, which would be modeled as an additive unwanted parameter [6]. The following discussion shows that this approach is only successful, but unwieldy, in the case of synchronized and noncoherent ACI, and fails in the more general unsynchronized scenario.

For simplicity in the discussion, let the received signal in AWGN and ACI be:

$$r(t) = s(t) + a(t) + n(t) \qquad (2.10)$$

where
$$s(t) = \sum_{j=1}^{N} b_j p(t - jT)$$

$$a(t) = \sum_{j=1}^{N} c_j p(t - jT - \lambda) \cos(2\pi f_d t + \theta) \qquad (2.11)$$

where b_i, c_i are independent equally likely (1 or -1) random variables, and the synchronization offset and the phase offset λ, θ are uniform independent random variables over (0,T) and (0,2π) respectively. The nuisance parameter approach is to assume a(t) is known in order to form f{ r | b, c, λ, θ } using the standard Karhunen-Loeve method for

AWGN. Then the desired f{ r | b } is obtained by averaging out the random parameters c, τ, θ according to the joint density function f{ c, λ, θ }= P{ c }f{ λ }f{ θ }. In equation form:

$$f\{ \mathbf{r}| \mathbf{b} \} = \sum_{i=1}^{N} P\{ c_i \} \int\int_{\lambda \ \theta} f\{ \lambda \} f\{ \theta \} f\{ \mathbf{r}| \mathbf{b},\mathbf{c},\lambda,\theta)d\theta d\lambda =$$

$$\sum_{i=1}^{N} \frac{P\{c_i\}}{(\pi No)^{1/2}} \int_0^T \int_0^{2\pi} \exp\left\{ -\frac{1}{No} \int_0^{NT} [r(t) - \sum_{j=1}^{N} b_i p(t-jT) + \sum_{j=1}^{N} c_j p(t-jT-\lambda) \cos(2\pi f_d t + \theta)\}]^2 dt \right\} d\theta d\lambda$$

(2.12)

The nuisance parameter approach results in the best average receiver in the case where theset of random (or nuisance) parameters are not estimated or detected. For the general case of an unsynchronized adjacent signal, this expression is not tractable for a realizable receiver. There is the complication of correlation between symbols due to time overlap of the adjacent signal's symbols, but more detrimentally is the non tractable (analytically) integral which does not provide the form for the sufficient statistics required by the receiver. In the case that the adjacent channel is synchronized (λ=0), this expression could be analyzed for a realizable receiver. This case is uninteresting, since if the adjacent channel is synchronized, then a noncoherently orthogonal modulation scheme for the two channels would be chosen resulting in no ACI.

2.4 Joint Maximum Likelihood Sequence Estimation

Joint maximum likelihood sequence estimation (JMLSE) is an optimum strategy for detecting both the SOI and the ACI in AWGN. The JMLSE receiver chooses one ensemble member of the SOI and ACI stochastic process that is closest in Euclidean distance to the received signal. Although JMLSE is not necessarily optimum for detecting

the SOI alone in AWGN and ACI, for the case where the cross-correlation between the SOI and the ACI is relatively weak, the performance can be very close to the performance of detecting the SOI in AWGN without ACI[7]. Since there is correlation between symbols, due to symbol overlap between adjacent channels because of the synchronization offsets, the JMLSE does not simplify to symbol by symbol detection. The main drawback for the JMLSE approach is the large increase in hardware , such as the additional phase lock loops, frequency oscillators and matched filters for detecting the adjacent channel signals. This increase in hardware may be prohibitive in some applications, such as battery powered hand held communication devices. Also there is some complexity involved in computing the JMLSE from the sufficient statistics with a dynamic programming algorithm such as the Viterbi Algorithm (VA).

One important feature of the JMLSE is its performance in the near-far effect, where the ACI is at a much higher power level than the SOI. Under the assumption that the phase and synchronization offsets of the ACI are known to the receiver, the JMLSE performance is neither limited and probably not even degraded, as is the case with the conventional matched filter receiver, by any relative increase in the power of the ACI. The JMLSE performance is not limited because there is no unbounded nuisance parameter due to the ACI as there is with the conventional receiver, since all of the ACI is estimated. In fact, with the increase in relative power of the ACI, the estimate of the ACI becomes more reliable. For the conventional receiver, however, an increase in ACI power means that the ACI at the output of the matched filter is more detrimental to performance. That the JMLSE performance may not even be degraded in the near far situation is suggested by some simulation studies of asynchronous CDMA systems detected by JMLSE [7]. The asynchronous CDMA system is analogous to ACI in the sense that each user's signal is weakly correlated with each other over all synchronization offsets. The results show that for the simple case of two CDMA signals there is an improvement in performance where, with an increase in the other user's signal power, the performance converges to that of

a single user. Note , however, that this discussion applies in the idealistic case where the phase and synchronization offsets of the ACI are known to the receiver. In practice, one associates a density function with the error of the estimates of synchronization and phase offsets $\hat{\lambda}$ and $\hat{\theta}$ which degrade the theoretical performance. The performance behavior of the JMLSE in the near-far effect should be confirmed under a realistic assumption for $f\{\hat{\lambda}\}$ and $f\{\hat{\theta}\}$.

Another difficulty with JMLSE for ACI in FDMA systems is exactly how much ACI should be jointly estimated. For example, should just the two closest adjacent channels be estimated, in which case there is some unestimated ACI , or should all the channels be estimated, which is prohibitively expensive in hardware. It is not clear that jointly estimating three channels in an unsynchronized FDMA system should have better performance for the SOI then simply detecting the SOI with a bandlimiting filter. One area where JMLSE has found application is in jointly estimating the SOI in cochannel interference, where the interference is localized in time and frequency with the SOI[8].

2.5 Subspace projection

Since the projection of the SOI and ACI onto a complete space is undesirable due to prohibitive receiver hardware and complexity, an alternative approach is to project onto a reduced subspace that is chosen according to an acceptable criterion. One problem is that there is no tractable criterion in the presence of ACI related to error performance. Note that for the case of stationary Gaussian ACI, the optimum filter (or equivalently the subspace) for the detection of the SOI is the whitened matched filter which also maximizes the signal power to interference power ratio (S/I). It is generally accepted that the best criterion in lieu of the ideal criterion is the subspace that maximizes the S/I . The difficulty, however, is in implementing this criterion, since the filtering is band limited which causes

both intersymbol interference and noise correlation. There is an inherent trade off between ACI rejection and ISI. The more bandlimited the filter is, the better the ACI rejection is, but the resulting ISI is more severe.

Because of the difficulties in implementing this criterion, there has only been one example where this criterion has been applied directly[9]. In this case the filtered received signal is sampled at the symbol rate and a decision feedback equalizer (DFE) is employed to reduce the resulting intersymbol interference. Other research has avoided ISI by optimizing a filter under the S/I criterion with the constraint that the filter has a limited time span[10]. Another study used[11] spectrally tighter filters but do not equalize the resulting ISI, since the increased ACI rejection more than offset this performance loss due to ISI.

In the last two decades there has been significant progress made in equalizing ISI resulting from the channel or transmitter filters. The two key areas are the DFE and the optimum MLSE approaches. Gains in ISI equalization are directly translated to gains in ACI rejection by allowing spectrally tighter filters at the front end of the receiver without comparative ISI loss. The rest of the chapter reviews how the DFE has been extended to combat ACI, and then presents a sub-optimum MLSE approach to combat ACI, which is the focus of this thesis.

2.5.1 DFE (Decision Feedback Equalization)

The DFE was originally devised as a modification to linear equalization of ISI channels. The DFE is composed of a forward filter, a sampler, and a decision threshold followed by a discrete feedback filter. The forward filter is designed to substantially frequency equalize the ISI, but with less noise enhancement than the perfect frequency equalization of the linear equalizer, with the residual ISI largely removed by the feedback

filter. Typically the forward and feedback filter are chosen according to the minimum mean square error criterion (MMSE) , which can be easily implemented adaptively using the least mean square algorithm (LMS).

The last decade has seen intense research into extending the DFE to combat ACI and co-channel interference(CCI) as well as ISI [2],[12]. Many simulation results confirm that fractionally spaced DFE, where the sampler samples atat least twice the signalling rate, is more robust than traditional MF receivers in suppressing ACI and CCI [13]. There are two explanations for the robust performance of fractionally spaced DFE. The first is that the sampled frequency response of the SOI is no longer aliased, and thus the forward filter can be more discriminating in suppressing interference, allowing the feedback filter to reduce the ISI. The second explanation is that choosing the forward filter under the MMSE criterion for two samples per symbol time exploits the cyclostationary nature of the interference. Since the SOI and the ACI are modulated signals, they are cyclostationary stochastic processes, where their mean and autocorrelation functions are periodic with time. Recent research has shown that the classical MMSE filtering (or Wiener filtering) for signals in interference can be extended to cyclostationary signals (or cyclic Wiener filtering) [14]. In the case of modulated signals, there is some gain in cyclic Wiener filtering compared to Wiener filtering, where the modulated signals are modeled as wide sense stationary by assuming the phase of the carrier is a uniform random variable. Forcing the forward filter to minimize the mean square error for two samples per symbol time means the forward filter more closely approximates the cyclic Wiener filter that minimizes the instantaneous (in time) mean square error, not the average mean square error (over a period in time) which the traditional Wiener filter implements. In the context of narrowband signals considered here, however, the gains in cyclic Wiener filtering are marginal [15] and also require that adjacent signals maintain a fixed phase and synchronization offset which is not the typical situation. However, in synchronous wideband systems such as CDMA, though, cyclic Wiener filtering (and sub optimum

implementations thereof) as a means to suppress CCI are proving to be a fertile research area [16].

One disadvantage of DFE is that the symbol by symbol hard decisions which are incompatible with soft decision decoding. Soft decision decoding, where a sampled version of the received signal is retained, is used for convolution codes, and trellis coded modulations in general. Although a form of DFE (Predictive Decision-Feedback Equalizer) has been designed for soft decision decoding, where the estimated bits from the decoding algorithm (usually the Viterbi algorithm) feed the feedback filter to reduce the ISI, the implementation is sub optimum since the forward and feedback taps are not jointly optimized under the MMSE criterion [17]. Another disadvantage is that the energy of ISI resulting from the forward filter is ignored in the detection of the signal. For signals in general, coded or uncoded, the ISI can be incorporated into the signal as a trellis and be detected using a soft-decision decoding algorithm for some detection gain.

2.5.2 Sub Optimum MLSE in AWGN and ACI

Maximum likelihood sequence estimation of signals in intersymbol interference is an optimum detection strategy. MLSE detection of signals in finite ISI is made tractable by modeling the ISI as a finite state machine (or equivalently a trellis) and evaluating the MLSE metric recursively using the Viterbi algorithm (V.A.) [18]. The MLSE approach was originally realized for linear modulations with a whitened matched filter which provided sufficient statistics as well as decorrelating the noise [19]. Recently the MLSE approach has been applied to trellis coded modulation (non linear modulations), whereby a bandlimited filter followed by a Nyquist sampler provides the uncorrelated sufficient

statistics [20]. For any given ISI channel, MLSE always performs better than DFE, because the MLSE uses the energy of the ISI for a detection gain. Depending on the nature of the ISI, the performance difference can be significant [17].

There has been no explicit work in using MLSE methods to combat ACI. Simmons proposed a bandlimiting trellis decoding receiver (BTR) using low pass filters followed by Nyquist samplers for continuous phase modulations (CPM) as a way to reduce the number of matched filters [21],[22]. The significant ISI terms are mapped onto the modulation trellis, which is then decoded by a trellis decoding algorithm such as the VA or M-algorithm. His work shows that with low pass filters of spectral roll off comparable to the CPM scheme, the BTR has the same ACI rejection capacity as the full matched filter VA receiver. The BTR can be extended to combat ACI directly, by choosing low pass filters with steeper spectral roll off than the matched filter which should provide better ACI rejection capacity without any ISI penalty in performance.

The focus of this thesis is to investigate the performance in AWGN and ACI of the BTR for MSK class modulations viewed as a linear offset quadrature modulation. The lowpass filters used are very close to the ideal brickwall filters. The BTR thus performs a MLSE of a bandlimited space in AWGN only. It should be the noted that the BTR can be easily extended to non linear modulation, such as the CPM example from Simmons' work.

3. THE BTR FOR MSK CLASS MODULATIONS

3.1 Introduction

This chapter initially discusses the class of MSK modulations in terms of the modulator, the optimum receiver in AWGN the quadrature matched filter , and the different types of MSK modulations with their respective spectral properties. The BTR is then developed in detail for the MSK class modulations, where the bandlimiting filter and the trellis decoding algorithm are presented for both cases of AWGN and AWGN with ACI.

3.2 MSK Class Modulations

Although MSK type modulations can be described as an example of a continuous phase modulation , where the continuity in the phase introduces memory into the signal, the discussion uses the alternative but equivalent model of linear quadrature constant envelope modulations. In this model, the transmitter divides the bit stream **a** into inphase and quadrature streams $\mathbf{a}^I$ and $\mathbf{a}^Q$, which linearly modulate the quadrature branches as shown in Figure 3-1 .

The transmitted signal s(t) is:

$$s(t) = A\sum_k a_k^I p(t - k2T_b)\cos(2\pi f_c t + \theta) + A\sum_k a_k^Q p(t - k2T_b - T_b)\sin(2\pi f_c t + \theta) \quad (3.1)$$

$$A = \sqrt{2E_b / T_b}$$

where the MSK type pulse p(t) satisfies the following constraints to ensure a constant envelope:

$$p(t) = p(-t) \quad\quad\quad\quad (3.2a)$$

$$p(t)^2 + p(t - T_b)^2 = 1 \quad t \in (0, T_b) \quad\quad\quad\quad (3.2b)$$
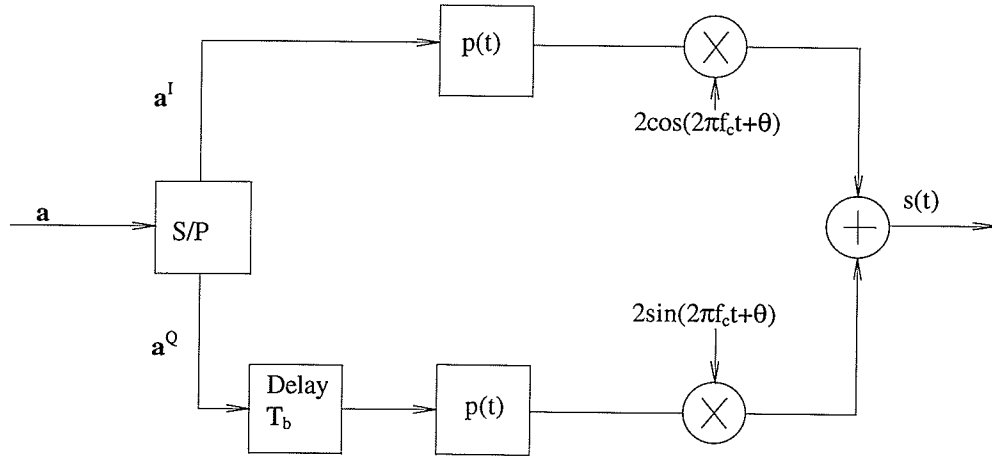
Figure 3-1 Parallel implementation of a MSK modulator

Note that the quadrature signals are interleaved by T_b in order to obtain the constant envelope.

For coherent modulation where θ is assumed to equal zero, it is convenient to express s(t) in terms of the baseband complex envelope $\hat{s}(t)$, where:

$$s(t) = \mathrm{Re}\left\{ \hat{s}(t) e^{j2\pi f_c t} \right\}$$ (3.3a)

$$\hat{s}(t) = A\sum_k a_k^I p(t - k2T_b) - jA\sum_k a_k^Q p(t - k2T_b - T_b)$$ (3.3b)

Three examples of MSK type modulations are offset quadrature phase shift keying (OQPSK), minimum shift keying (MSK) and sinusoidal frequency shift keying (SFSK). Their pulse shapes have the following form:

$$\text{OQPSK: } p(t) = \frac{1}{\sqrt{2T_b}} \qquad -T_b \le t \le T_b$$ (3.4a)

$$\text{SFSK: } p(t) = \frac{1}{T_b}\cos\left(\frac{\pi t}{2T_b} - \frac{1}{4}\sin\left(\frac{2\pi t}{T_b} \right) \right) \qquad -T_b \le t \le T_b$$ (3.4b)

20
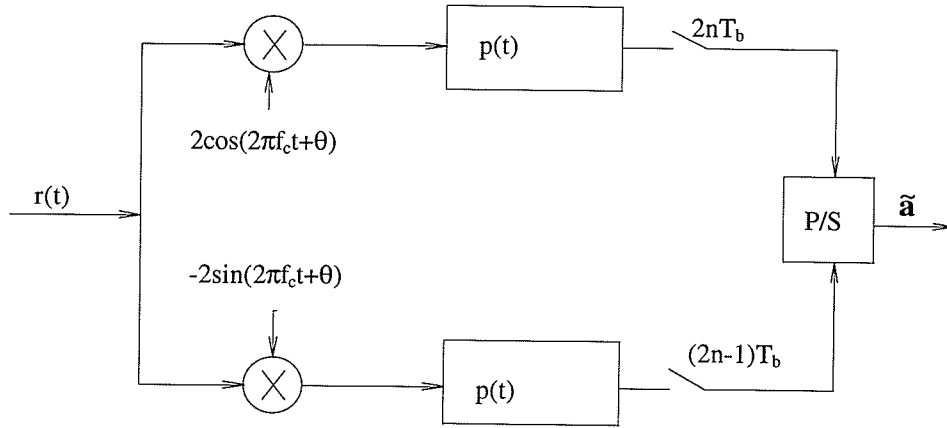
Figure 3-2 Quadrature Correlation filter for MSK modulations

$$\text{MSK: } p(t) = \frac{1}{T_b}\cos\left(\frac{\pi t}{2T_b}\right) \qquad -T_b \le t \le T_b \qquad (3.4c)$$

3.2.1 Performance in AWGN

The optimum receiver for MSK modulations in AWGN is the quadrature correlation receiver as shown in Figure 3-2. The quadrature correlation receiver performs matched filtering on each quadrature symbol. The symbol decisions in each branch are statistically independent from each other because with reasonable f_c the quadrature matched filters are effectively orthogonal to each other. Under the assumption of equally likely independent bits , the probability of bit error (P_b) is two times the probability of symbol error (P_e) minus the square of the probability of symbol error.

This probability of bit error P_b of power spectral density No/2 watts/Hz is given by:

$$P_b \cong 2Q\left(\sqrt{\frac{2E_b}{No}}\right) \qquad (3.5)$$

where:

$$Q(x) = \frac{1}{\sqrt{2\pi}}\int_x^\infty \exp\left(-\frac{x^2}{2}\right)dx. \qquad (3.5b)$$

3.2.2 Bandwidth Properties.

The bandwidth properties are analyzed in terms of the average power density spectrum (PDS) of the modulated signals. According to the Wiener-Khintchine Theorem, if s(t) is wide sense stationary, then the PDS is obtained from the Fourier transform of the autocorrelation function. When the phase of the carrier is assumed unknown and modeled as a uniform random variable, then the modulated signal is considered wide-sense stationary. Typically the modulated signal is viewed from a non coherent standpoint, say an adjacent channel, and hence the wide-sense stationary model is used here. Note if the phase of the carrier is known then the modulated signal is cyclostationary, where the mean and the autocorrelation function are periodic in time.

Since s(t) is a passband process, the PDS of s(t), $\mathbf{S}(f)$, is related to the PDS of the complex baseband envelope $\hat{s}(t)$, $\mathbf{S}_c(f)$, by:

$$\mathbf{S}(f) = \frac{1}{4}\left(\mathbf{S}_c(f - f_c) + \mathbf{S}_c(-f - f_c)\right) \tag{3.6}$$

For the MSK modulations, the autocorrelation function $R(\tau)$, which is the expected value of the product $\hat{s}(t)(s(\hat{t} + \tau))^*$ is:

$$R(\tau) = E_{a^I, a^Q}\left(\begin{array}{l} (A\sum_k a_k^I p(t - k2T_b) - jA\sum_k a_k^Q p(t - k2T_b - T_b)). \\ (A\sum_i a_k^I p(t - k2T_b + \tau) + jA\sum_k a_k^Q p(t - k2T_b - T_b + \tau)) \end{array} \right) \tag{3.7}$$

Since $\mathbf{a}^I$ and $\mathbf{a}^Q$ are sequences of statistically independent (+/- 1) random variables, $R(\tau)$ simplifies to:

$$R(\tau) = \frac{A^2}{T_b} \int_{-2T_b}^{2T_b} p(t)p(t + \tau)dt \tag{3.8}$$

22
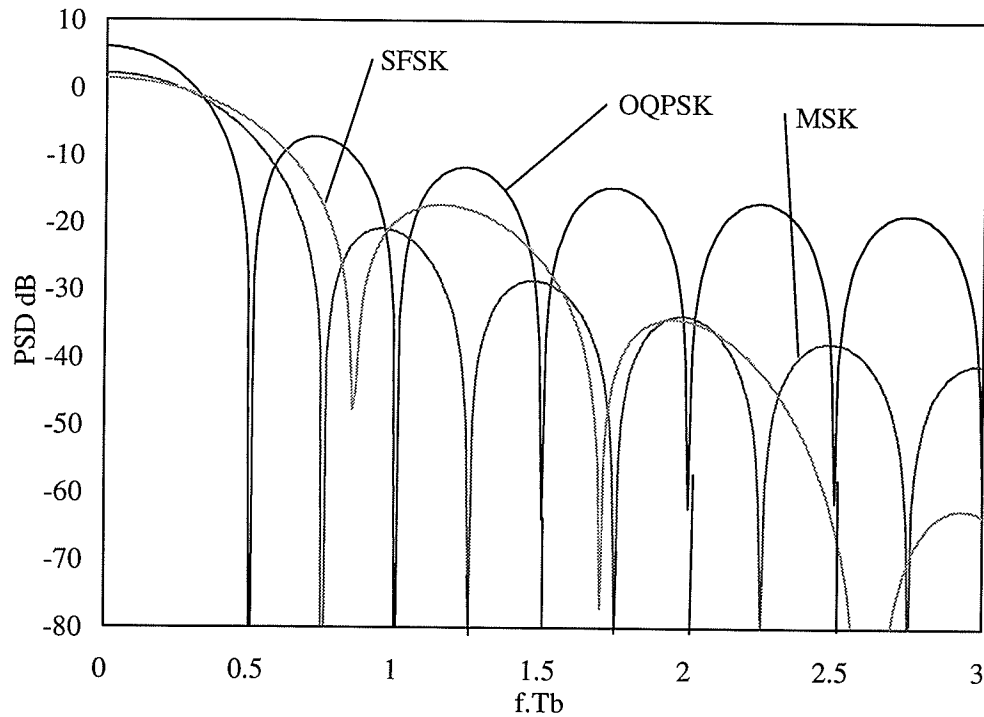
Figure 3-3 PDS of OQPSK, SFSK, and MSK

Therefore, the PDS of the complex envelope $S_c(f)$ is:

$$S_c(f) = \frac{A^2}{T_b}|P(f)|^2 \quad \text{watts/Hz} \qquad (3.9)$$

$$\text{where } P(f) = \int_{-\infty}^{\infty} p(t)e^{j2\pi ft}dt.$$

Hence the spectral properties of the MSK modulation are directly tied to the spectral properties of the pulse shape. Figure 3-3 shows the PDS of the complex envelopes for these three modulations. The asymptotic spectral roll off decays at the rate of $1/f^{2n+2}$, where n is the number of times the pulse can be differentiated before the end points become discontinuous. Hence the PDS of OQPSK decays at $1/f^2$, MSK decays at

$1/f^4$, and SFSK decays at $1/f^6$. Notice that for modulations with sharper spectral decay, there is a corresponding larger main lobe in the PDS due to the increased concentration of signal power in the main lobe. With this brief discussion of the transmitter implementation for MSK class modulations and their properties, the BTR for this class of modulations is presented next.

3.3 BTR model for MSK modulations

3.3.1 Overview

The received signal r(t) in AWGN is:

$$r(t) = s(t) + n(t) \tag{3.10a}$$

where $s(t) = A \sum_k a_k^I p(t - k2T_b) \cos(2\pi f_c t) + A \sum_k a_k^Q p(t - k2T_b - T_b) \sin(2\pi f_c t)$ (3.10b)

$$A = \sqrt{2E_b / T_b}$$

and n(t) is white Gaussian noise with two sided spectral density No/2 watts/Hz. In each quadrature arm, the BTR receiver consists of a bandlimiting filter h(t), sampler, and trellis decoder. Each trellis decoder estimates the respective bit stream which are then de-interleaved to form an estimate of the original bit stream. The receiver model is shown in
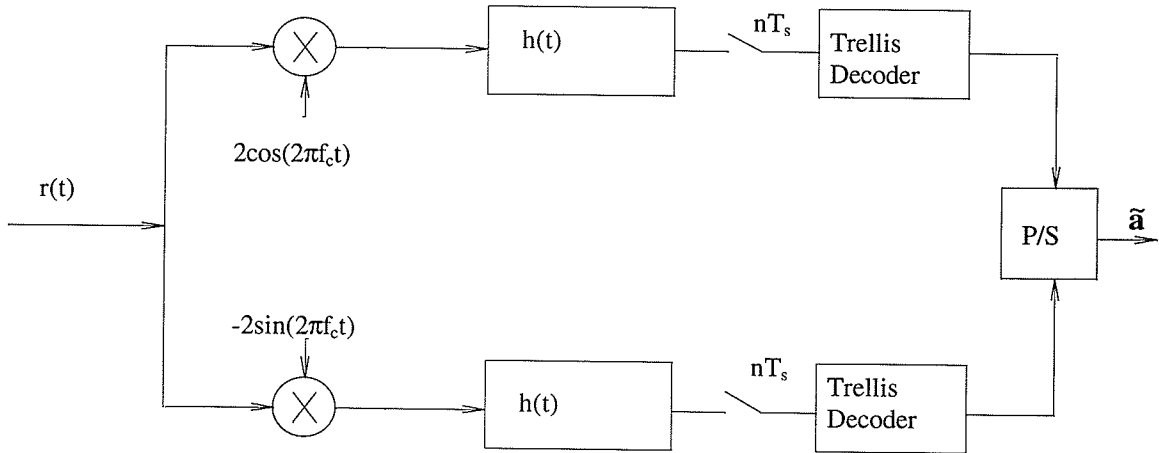
Figure 3-4 BTR receiver for MSK modulations

24

Figure 3- 4.

3.3.2 Bandlimiting filter

The important factors concerning the choice of the bandlimiting filter h(t) are the steepness of the spectral roll off and the effect on the noise statistics. The spectral roll off must be considerably steeper than of the matched filter, otherwise there is no relative benefit in ACI rejection. For ease in implementing the trellis decoding, it is desirable that the samples be very close to being statistically independent . For AWGN, the Power Density Spectrum of the noise at the output of the filter is proportional to $|H(f)|^2$. If $|H(f)|^2$ is proportional to a Nyquist form, then Nyquist sampling of the output will result in uncorrelated samples, which because they are Gaussian random variables will be statistically independent. In consideration of these factors, the following filter was chosen:

$$h(t) = \sin(2\pi W(t - 7.5T_{sy})) / (\pi(t - 7.5T_{sy})) \quad 0 \le t \le 15T_{sy} \qquad (3.11)$$
$$= \quad 0 \quad \text{elsewhere}$$

The bandlimiting filter h(t) approximates the ideal brick wall filter with impulse response $\sin(2\pi Wt)/\pi t$ with bandwidth W, but truncated to 15 T_{sy} , with a delay of 7.5 T_{sy} to make it causal. Two bandwidths are considered , $W=0.5/T_b$ and $W=0.25/T_b$. Note that $T_{sy}=2T_b$ because of the quadrature modulation. The two chosen bandwidths have Nyquist sampling rates which are commensurate with T_{sy}. Although the sampling rate need not be commensurate with T_{sy} for implementation, this feature makes synchronization as well as the trellis decoding easier to perform. Note that $W=0.5/T_b$ corresponds to the
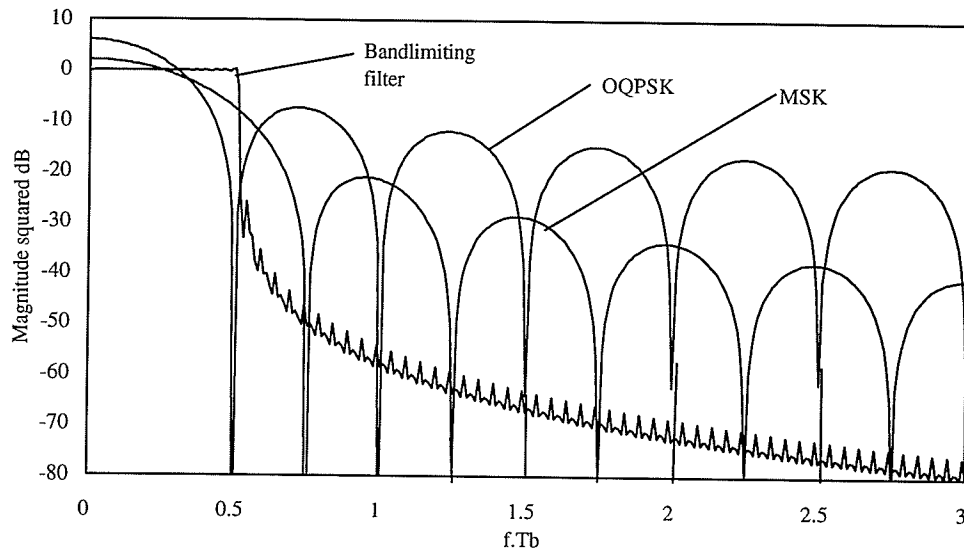
Figure 3-5 Magnitude squared spectral responses for the bandlimiting filter with W=0.5/T$_b$, and for the matched filters of OQPSK and MSK

97% in band power bandwidth for MSK, where as W=0.25/T$_b$ corresponds to 69%.

In order to check that the filter has a narrower spectral roll off then the matched filters, Figure 3-5 shows the magnitude squared spectral response of the matched filters for OQPSK and MSK compared to $|H(f)|^2$. Figure 3-5 shows that indeed h(t) with W=0.5/T$_b$ has a steeper roll off than the matched filter. For the case with W=0.25/T$_b$, h(t) has the same roll off as indicated by Figure 3-5 but the main lobe is narrower. One way to quantify the difference between the ideal bandlimited filter and the approximation is to compare the amount of power due to an adjacent signal that each filter passes. For one adjacent MSK signal frequency spaced by 2/T$_b$ with W=0.5/T$_b$, the filter allows 0.006 dB more adjacent channel interference (ACI) power than an ideal bandlimited filter. Note for this spacing that the matched filter allows 2.57 dB more ACI power than the ideal filter.

The correlation between noise samples due to the AWGN at the output of h(t) is
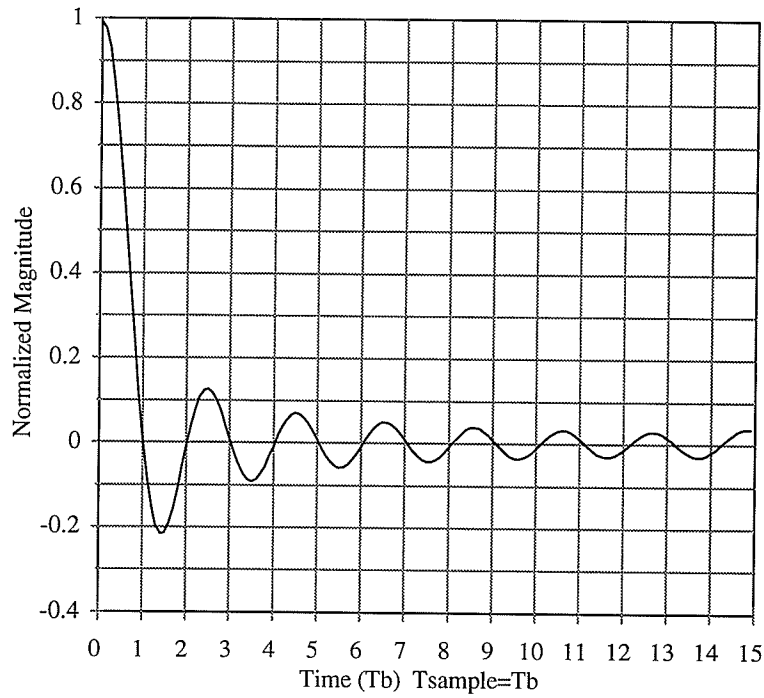
Figure 3-6 Normalized filter autocorrelation function with
W=0.5/T$_b$

determined by the autocorrelation function $R_h(\tau)$:

$$R_h(\tau) = \int h(t)h(t+\tau)dt \qquad (3.12)$$

Figure 3.6 shows the normalized autocorrelation of h(t) with W=0.5/T$_b$. For W=0.25/T$_b$, the autocorrelation function has same form except it is scaled by 2T$_b$.The figure shows that correlation values between Nyquist sampling times (n/T$_s$ n≠0) are approximately zero and can in effect be considered uncorrelated. Since the noise samples are Gaussian, these samples can be considered statistically independent.

The structure of the ISI at the output of the filter with the two bandwidths due to
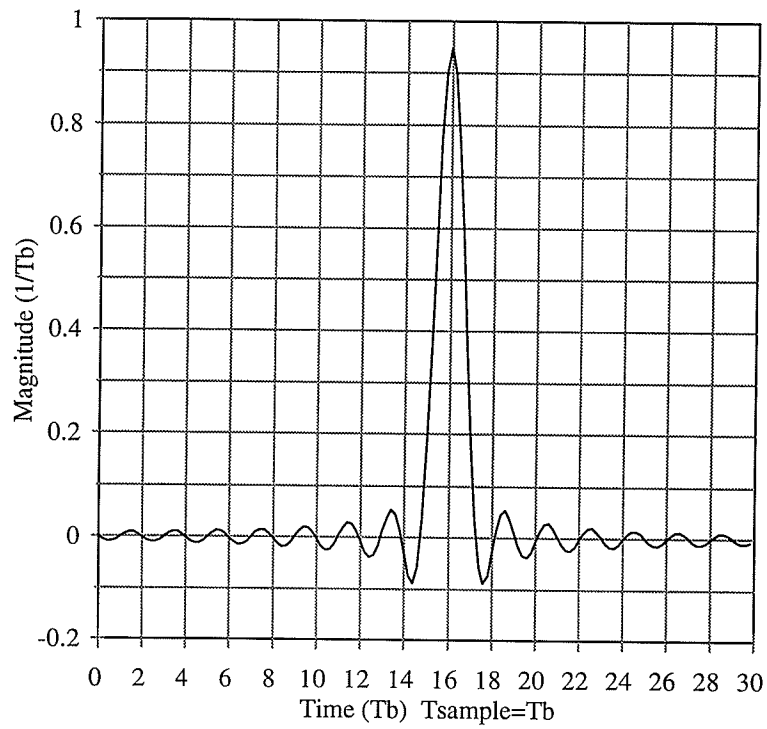
Figure 3-7 Output of h(t) with W=0.5/Tb due to MSK pulse
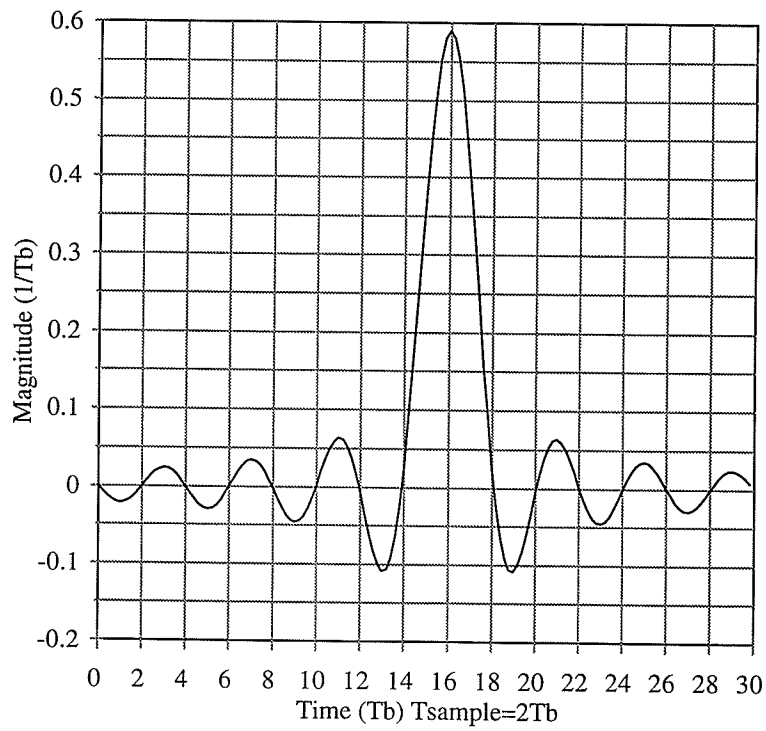
Figure 3-8 Output of h(t) with W=0.25/Tb due to MSK pulse
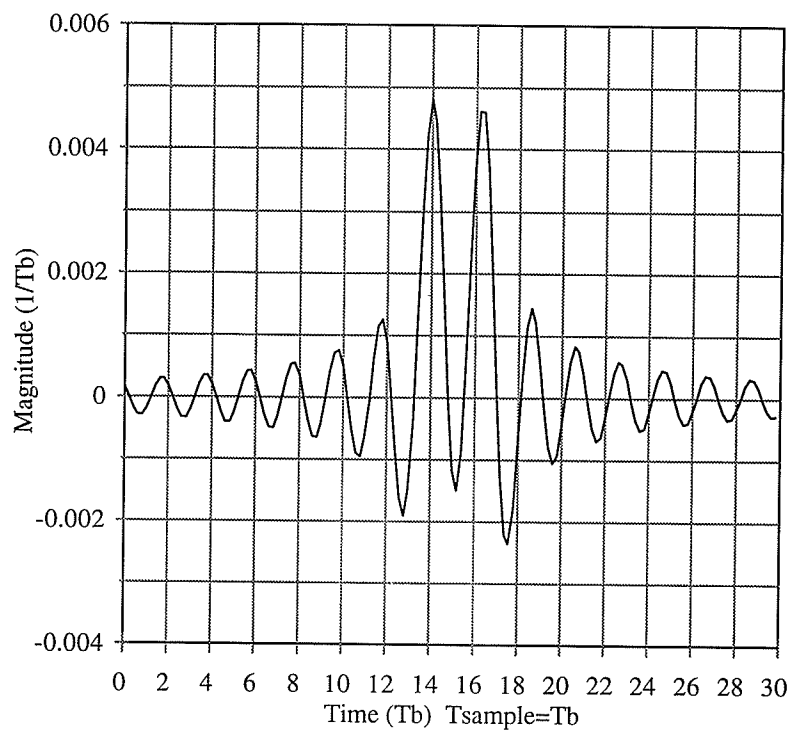
Figure 3-9 Output of h(t) with W=0.5/Tb due to adjacent MSK pulse frequency offset by 2/Tb
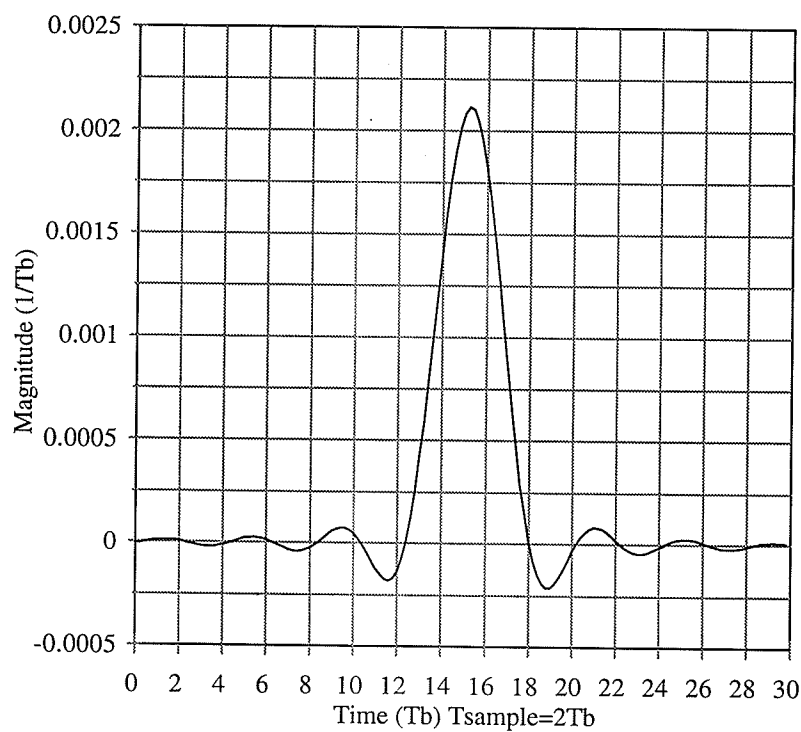
Figure 3-10 Output of h(t) with W=0.25/Tb due to adjacent MSK pulse frequency offset by 2/Tb

29

one MSK pulse is shown in Figures 3-7 and 3-8. The samples at the Nyquist sampling times, except for two symbol intervals from 14-18 T_b, are approximately zero for the two cases. Although the filter's impulse has length of 15 T_{sy}, there is only ISI for one symbol length when Nyquist sampled. One explanation is that the filtered signals spectrum is approximately flat over the limited bandwidth, particularly for $W=0.25/T_b$, which thus approximates the flat bandlimited spectrum of a Nyquist pulse. From an energy standpoint point, the samples from these two symbol intervals represent over 99.99% of the total energy of the filtered signal for all the modulations considered.

The structure of a filtered adjacent signal pulse is contrasted to the filtered signal of interest (SOI) pulse. Figure 3-9 shows the output of h(t) with $W=0.5/T_b$ due to one adjacent MSK pulse with a frequency offset by $2/T_b$. This filtered pulse's energy is more spread out over the time axis, which gives rise to more significant ACI terms. The structure of this filtered pulse only depends on the bandwidth of the filter, since the synchronization offset simply shifts this filtered pulse in time, where as the phase and frequency offset modify the magnitude of this filtered pulse. Figure 3-10 shows the output of h(t) with $W=0.25/T_b$ due to one adjacent MSK pulse with a frequency offset of $2/T_b$. Here the filtered output is a pulse, approximately half cosine in shape, which extends over 3 symbol lengths. Note that the magnitude of this pulse is dependent on the random phase offset parameter. The trend with even narrower filtering is to elongate this pulse over the time axis. Again this filtered pulse has more significant ACI terms than for the corresponding filtered SOI pulse.

3.3.3 Sufficient Statistics

Assuming that the filtered signal is ideally bandlimited to W, then the signal can be uniquely represented by a linear combination of the orthogonal basis set for W bandlimited space, which is $\{\sin(2\pi W(t-n/2W))/\pi(t-n/2W)\}$ where $n \in Z$. These basis functions have the property that at $t=n/2W$ all other basis functions equal zero except the function which has been translated by $n/2W$ from the origin. Hence sampling at 2W, the Nyquist rate, provides sufficient statistics to the trellis decoder, since the original bandlimited signal can be reconstructed from these samples.

Since the samples are the coefficients of orthogonal bases set, the Euclidean distance between two filtered signals, say $s_1(t)$ and $s_2(t)$, can be computed in terms of their samples $\{s_{1i}\}$ and $\{s_{2i}\}$. Thus,

$$\left\| s_1(t) - s_2(t) \right\|^2 = \frac{1}{2W} \sum_i (s_{1i} - s_{2i})^2 \tag{3.13}$$

3.4 Trellis Decoder.

3.4.1 Trellis Description in AWGN

Trellis description of ISI follows when the ISI resulting from the causal bandlimiting filter h(t) is modeled as a finite state machine. To develop the trellis consider first the sampled vector $\mathbf{z}^I$ of the inphase filter ouput the $j^{'\text{th}}$ symbol interval:

$$\mathbf{z}_j^I = \sum_{k=0}^{L} a_{j-k}^I \mathbf{g}_k + \mathbf{n}_j^I \tag{3.14}$$

where $g_{k,i} = g(t = kT_{sy} + iT_s) = \int_{-\infty}^{\infty} p(t - \tau - T_b)h(\tau)d\tau$, L is the memory length in units of T_{sy} of the filter, $\mathbf{n}_j^I$ is the sampled noise of variance 2NoW watts, and $\{\mathbf{g}_k\}$ is the sampled impulse response of the overall channel. Note that a state is defined over T_{sy} not T_s, and hence the channel coefficients $\{g_i\}$, noise input $\mathbf{n}_j$, and output z_i are [1xS] vectors where S is equal to T_{sy}/T_s. The memory vector of the channel defines the state and
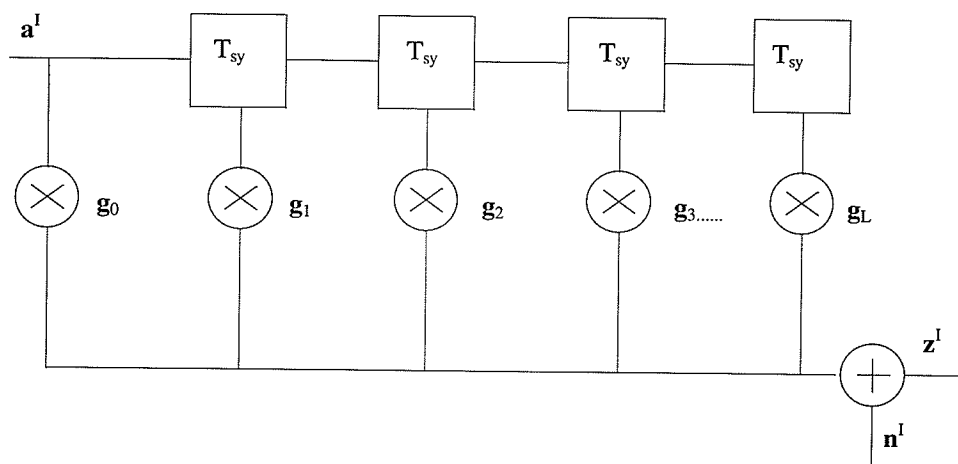
Figure 3-11 Finite state machine model of intersymbol interference

the number of states equals 2^L. The state is defined for the whole symbol length T_{sy} because the transitions of this finite state machine occur every T_{sy}. Figure 3-11 shows the finite state machine model of the causal bandlimiting filter.

A trellis comprises of defining the mappings from an information vector $\mathbf{a}^I$ of length L to a set of discrete output vectors { s_i }, as well as the allowable transitions between the states which are defined by L information symbols. In this case, the finite state machine model of the ISI provides both the set of mappings and allowable transitions sufficient for a trellis description. The trellis is shown in Figure 3- 12, where the memory length is 2.

3.4.2 Decoding the Trellis in AWGN

The maximum likelihood sequence estimation (MLSE) method for estimating the information sequence (vector) $\mathbf{a}^I$ given the received vector $\mathbf{z}^I$ is to choose the $\mathbf{a}^I$ that maximizes the conditional probability P{ $\mathbf{z}^I | \mathbf{a}^I$ }. In order to evaluate P{ $\mathbf{z}^I | \mathbf{a}^I$ }, the statistics of noise vector $\mathbf{n}^I$ are required. For the case of AWGN, the statistics of $\mathbf{n}^I$ are known. They are identical independent Gaussian random variables with zero mean and a variance of 2NoW watts. For a block length Ns, the MLSE rule chooses $\mathbf{a}^I$ that maximizes the total metric:
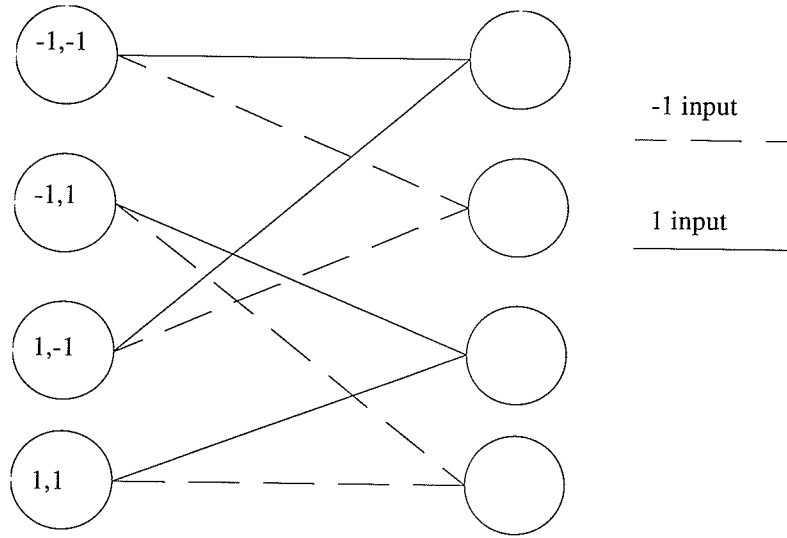
Figure 3-12 Trellis with L=2

$$\ln[P\{\ \mathbf{z}^I \big| \ \mathbf{a}^I\ \}] = -\sum_{j=1}^{Ns} \left\| \mathbf{z}_j^I - \sum_{k=0}^{L} a_{j-k}^I \mathbf{g}_k \right\|^2 \tag{3.14}$$

Note that $\mathbf{z}_j^I$ and $\mathbf{g}_k$ are 1xS vectors, and the metric in (3.14) is defined over $\Re^S$ .The sum in equation (3.14) is the total metric for a given sequence $\mathbf{a}^I$. The individual terms due to each output transition in the total metric are called branch metrics. At each transition there are only 2^L possible branch metrics, since the information symbols are binary. Without any simplification, to compute the total metric for all possible sequences would require a prohibitive 2^{Ns} computations. The Viterbi Algorithm, however, dramatically reduces the number of computations by exploiting the trellis description to compute the total metric.

3.4.3 The Viterbi Algorithm

There is a wealth of literature on the VA, particularly as a means to implement MLSE for linear ISI channels[19] . A brief discussion of the VA follows, in order to

highlight the basic assumptions by which the VA works. The VA searches the trellis for the most likely path according to the following steps.

1) The VA keeps one survivor path at each state, while retaining the accumulated metric of that path. Hence there are 2^L survivor paths kept at each iteration..

2) For the next iteration, the VA extends these 2^L survivor paths to 2^{L+1} paths and computes the new accumulated metrics of these 2^{L+1} paths by adding the new branch metric to each.

3) At each state, the VA then rejects the path with the smaller metric, and hence retains 2^L new survivor paths with their new accumulated metrics.

The above is repeated until end of block is reached. The survivor path with the largest accumulated metric is then chosen

Note that the VA requires $Ns2^L$ computations compared to the brute force 2^{Ns} . The key idea of the VA is that if two paths merge in a trellis state, then the path with the smaller metric can be rejected because any two signals which have the same signal component after the merge, the signal whose 'tail' has a larger metric will always be larger. The main assumption behind this idea is that future metrics are independent of present and past metrics. More generally, future received samples are statistically independent of present and past received samples, and hence knowledge of future samples does not change the likelihood of present and past samples. In the case of AWGN and the causal bandlimiting filter with [H(f)] very close to Nyquist 1 form, the received samples are statistically independent and thus the VA effectively performs MLSE .

3.4.4 Truncated ISI

Recall that for the chosen filter the total ISI spans 15 symbol lengths, with over 99.9 % of the total energy contained in three symbol lengths. The trellis decoder ignores

all the other ISI terms except from the 3 symbol lengths mentioned, which gives the trellis a memory length of two (L=2). The residual ISI is an amplitude bounded random variable which is below -30 dB power relative to the signal power ; hence it has minimal to no effect on performance.

3.5 Trellis Decoder In AWGN and ACI

In order to understand the impact of the filtered ACI in the decoding of the ISI trellis of the signal of interest (SOI), it is necessary to examine the structure of this ACI to estimate its first and second order statistics. In the presence of ACI, the received signal at the front end of the receiver is:

$$r(t) = As(t) + a(t) + n(t) \tag{3.16a}$$

where
$$a(t) = \sum_{i=1}^{Na} \sum_{j} A_i a_{i,j}^I p_i(t - j2T_b - \lambda_i) \cos(2\pi f_i t + \theta_i)$$

$$- \sum_{i=1}^{Na} \sum_{j} A_i a_{i,j}^Q p_i(t - j2T_b - T_b - \lambda_i) \sin(2\pi f_i t + \theta_i) \tag{3.16b}$$

is the ACI signal, Na is the number of interferers, $\{A_i, f_i, \lambda_i, \theta_i\}$ are the parameters of each interferer, and λ_i, θ_i are independent uniform random variables over $(0,2\pi)$, $(-T_b,T_b)$ respectively. It is assumed that all the inphase and quadrature bit streams of the interferers are independent equally likely random variables. For the inphase trellis decoder, then the sampled signal for the j'th symbol time is:

$$\mathbf{z}_j = \mathbf{s}_j + \sum_{i=1}^{Na} \mathbf{AI}_{i,j} - \sum_{i=1}^{Na} \mathbf{AQ}_{i,j} + \mathbf{n}_j \tag{3.17a}$$

$$\mathbf{AI}_{i,j} = A_i \sum_{k=1}^{N} a_{i,j-k}^I \mathbf{g}_{i,k}^I, \quad \mathbf{AQ}_{i,j} = A_i \sum_{k=1}^{N} a_{i,j-k}^Q \mathbf{g}_{i,k}^Q \tag{3.17b}$$

$$g_{i,j}^I = g^I(t = iT_{sy} + jT_s) = \int_{-\infty}^{\infty} p(\tau - T_b - \lambda_i) \cos(2\pi(f_i - f_c)\tau + \theta_i) h(t - \tau) d\tau \tag{3.17c}$$

$$g_{i,j}^Q = g^Q(t = iT_{sy} + jT_s - T_b) = \int_{-\infty}^{\infty} p(\tau - T_b - \lambda_i) \sin(2\pi(f_i - f_c)\tau + \theta_i) h(t - \tau) d\tau \tag{3.17d}$$

where $\mathbf{AI}_{i,j}$, $\mathbf{AQ}_{i,j}$ are 1xS vectors of the inphase and quadrature interference due to the i'th interferer.

3.5.1 First Order Statistics

Since the filtered adjacent signal is time dispersed, the sample value due to the filtered ACI is a sum of independent equally likely random variables each multiplied by a coefficient of approximately the same magnitude. For one interferer, there are two sets of terms due to the inphase and quadrature interference. For the case with $W=0.5/T_b$, there are approximately 30 terms, and with $W=0.25/T_b$, there are approximately 6 terms, as previously indicated for one interferer. By invoking the central limit theorem, it is a reasonable assumption that the sampled filtered ACI in both cases, but particularly with $W=0.5/T_b$, tends to a first order density Gaussian random variable. Note this assumption is even truer in the presence of more than one interferer of the same relative power.

One way to check the accuracy of this Gaussian approximation is to estimate the first order density function by a Monte Carlo simulation. The two examples examined are one MSK adjacent signal with a frequency offset by $2/T_b$ and filtered with $W=0.5/T_b$ and $W=0.25/T_b$.

The estimate of the density function is based on the histogram method. The range of the samples is divided into equal sized bins, and the estimate of the probability at the center of a bin is simply the number of samples falling in that bin divided by the product of the total number of samples and the bin size. The number of bins used here is 200.

The density estimate of the filtered ACI with $W=0.5/T_b$ in Figure 3-13 is shown to be very close to a Gaussian density with the same variance, which verifies in this case that the Gaussian approximation is reasonable . To check the robustness of this assumption, the same Monte Carlo density estimate of the filtered ACI was run for the case of one interferer, with frequency offsets of $2.0/T_b$, $1.5/T_b$, $1.0/T_b$. The results showed the density estimate had the same form for all cases, which is expected since the frequency spacing only modifies the magnitude of the filtered adjacent signal pulse and does not change its form. The density estimate for $W=0.25/T_b$ in Figure 3-14 only
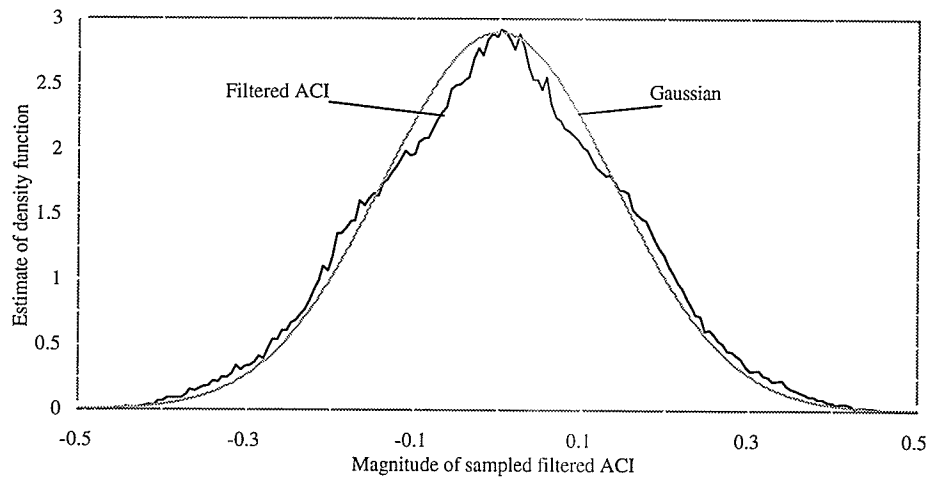
Figure 3-13 Estimate of amplitude density of filtered MSK pulse frequency offset at 2.0/Tb with W=0.5/Tb at 23 dB interference power to signal power, and Gaussian density with same variance as filtered ACI.
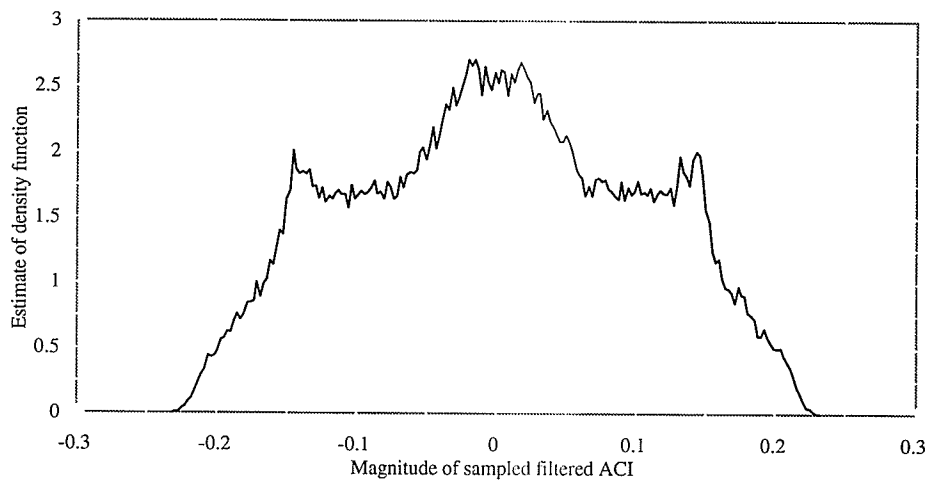

Figure 3-14 Estimate of amplitude density of filtered adjacent MSK pulse frequency offset at 2.0/Tb with W=0.25/Tb at 23 dB interference power to signal power

approaches the form of a Gaussian density, since there are significantly less terms of the filtered adjacent signal pulse.

3.5.2 Second Order Statistics.

The approach taken here is to model the filtered ACI as white Gaussian noise. The advantage of this approach is that the receiver does not require knowledge of any parameter of the ACI. The accuracy in this model of filtered ACI as additive white Gaussian noise is examined later in the simulations. There may be benefit, however, in modeling the filtered ACI as colored Gaussian noise, where this interference spectrum is given by the power density spectrum of the filtered ACI. In order to whiten this interference noise, however, the receiver needs to know the relative power level of the AWGN and the filtered ACI. In addition, there may be some benefit in exploiting the statistical dependence between quadrature branches which exist because of the ACI. The trellis decoder thus performs a sub optimum MLSE by modeling the filtered ACI as AWGN, hence requiring no changes in its metrics from the case of no ACI.

3.6 Summary

The MSK class modulation has been described as a class of constant envelope linear offset quadrature modulation. The matched filter is shown as optimum in the presence of AWGN only. The BTR was developed for the MSK class modulations, where the received signal is projected onto a bandlimited subspace by the filter followed by Nyquist sampler, and then processed by a trellis decoder. The BTR performs a MLSE on the bandlimited subspace in AWGN , and performs a sub optimum MLSE in the presence of ACI by modeling the filtered ACI as AWGN. The next chapter investigates the performance both analytically and with simulations of the BTR compared with the matched filter in AWGN and in ACI.

4. BTR PERFORMANCE IN AWGN AND ACI

The performance of the BTR in the cases of AWGN and with ACI are investigated both analytically and by simulation. This performance shows that the BTR has comparable performance with the optimum matched filter (MF) in the case of AWGN. In addition, the BTR is compared with a simpler receiver (SR) with no trellis decoder which samples the filtered signal every symbol interval. The BTR is shown to have a performance gain relative to the SR by exploiting the energy of the samples not detected by the SR as well as avoiding degradation due to any residual ISI. For the case of ACI, the BTR has significant performance gain up of to 4.8 dB compared to the MF. The programs for the simulations were written in C and were executed on a Sun workstation.

4.1 BTR PERFORMANCE IN AWGN

The performance of the BTR compared to the MF in AWGN is investigated both analytically and with simulations for OQPSK, MSK and SFSK . The analysis indicates that for these modulations there is negligible degradation in minimum distance for the BTR with $W=0.5/T_b$, but with $W=0.25/T_b$ there is from 1.11 dB to 2.15 dB degradation depending on the modulation. Monte Carlo simulation which exactly model the channel conditions verify the results of the analysis.

4.1.1 Error Analysis

For moderate to high SNR, the error performance of the trellis decoder is determined by the minimum Euclidean distance between any two signal sequences. Since the two quadrature trellis decoders are identical and independent in AWGN, the analysis is restricted without loss of generality to the inphase trellis decoder. Since the channel for

the inphase decoder is a linear intersymbol channel, the difference signal between any two possible signal sequences is equivalently the signal modulated by the difference sequence (or error sequence) of those two inphase information sequences [27]. In general, depending on the severity and type of intersymbol interference, the determination of the error sequence that gives rise to the minimum distance is very difficult. Here, however, it is reasonable to propose, that since the channel filter has no spectral nulls and the trellis has memory length of 2, the minimum error sequence is 2,0,0,....This proposition is verified later by computer simulations.

The probability of error event (P_e) for the inphase trellis decoder at moderate to high signal to noise ratio is:

$$P_e \cong Q(\sqrt{d_{min}^2 E_s / 4\sigma_n^2})$$ (4.1)

where d_{min}^2 is the normalized minimum distance squared, E_s is the energy of the minimum difference signal, and σ_n^2 is the variance of the AWGN which is No/2 watts. In the sampled domain, d_{min}^2 caused by the error sequence 2,0,... is calculated by:

$$d_{min}^2 = \frac{1}{2W}\sum_{j=1}^{L}\|2\mathbf{g_i}\|^2 = \frac{2}{W}\sum_{j=1}^{L}\|\mathbf{g_i}\|^2$$ (4.2)

where $g_{i,j} = g(t = iT_{sy} + jT_s) = \int_{0}^{T_{sy}} p(\tau - T_b)h(t - \tau)d\tau$. Recall that: $\int_{-\infty}^{\infty} p(t)^2 dt = 1$.

The factor 1/2W normalizes d_{min}^2 to unit energy and thus the baseband noise variance to No. Since the residual ISI is less than -30 dB, then

$$\frac{1}{2W}\sum_{i=0}^{L}\|\mathbf{g_i}\|^2 \cong \int_{-W}^{W}|P(f)|^2 df$$ (4.3)

where $P(f) = \int_{-\infty}^{\infty} p(t)\exp(-i2\pi ft)dt$. Hence d_{min}^2 equals:

$$d_{min}^2 = 4 \int_{-W}^{W} |P(f)|^2 \, df \tag{4.4}$$

Recall that without ISI, where the optimum performance in AWGN is achieved with the MF, d_{min}^2 equals 4. Thus the performance degradation of d_{min}^2 in dB for the inphase trellis decoder compared to the MF performance in AWGN is :

$$10 \log(\int_{-W}^{W} |P(f)|^2 \, df) \quad dB \tag{4.5}$$

Equation (4.5) indicates that the more bandwidth efficient the MSK pulse is in terms of minimizing the out of band power radiation at a particular bandwidth W, the smaller the corresponding performance degradation is for the BTR. Table I shows d_{min}^2 dB losses calculated for OQPSK, MSK, SFSK with $W=0.5/T_b$, and $W=0.25/Tb$ respectively.

Table I BTR d_{min}^2 loss in dB for $W=0.5/T_b$, and $W=0.25/T_b$ compared to MF.

	$W=0.5/T_b$	$W=0.25/T_b$
OQPSK	0.457 dB	1.114 dB
SFSK	0.342 dB	2.147 dB
MSK	0.132 dB	1.561 dB

The degradation factor shows that the BTR performance is sensitive to bandwidth. For narrow bandwidths, such as $0.25/T_b$, even though the AWGN is narrowly filtered, there is a net performance degradation dependent on the bandwidth. This feature suggests that a BTR with a narrow bandwidth ($0.25/T_b$) compared to a wider bandwidth ($0.5/T_b$) may not be as good at rejecting ACI because of the poor trade off between the reduction of interference power and the reduction in d_{min}^2. This trend is demonstrated when the performance of the BTR in AWGN and ACI is considered.

As an interesting aside, Wittke and Deshpande [1] have determined the optimum MSK type pulses according to the criterion of minimizing the out of band radiation for a

particular bandwidth W. Of interest is that their research reveals that for the bandwidth $W=0.5/T_b$ the MSK pulse is very close to the optimum, whereas for $0.25/T_b$ OQPSK is close to optimum.

Note that since the AWGN is uncorrelated and hence statistically independent in each quadrature branch, then the probability of error event (P_e) in the inphase trellis decoder is independent of the probability of error event in the quadrature trellis decoder (which has the same probability). Each error event has 1 bit in error. Thus the overall bit error rate P_b equals:

$$P_b = 2P_e - (P_e)^2 \cong 2P_e. \qquad (4.6)$$

4.1.2 Simulation Results

Simulations were conducted according to an exact baseband model of the inphase trellis decoder . Hence all the ISI terms (even those discarded by the trellis decoder) are simulated, and the noise samples are uncorrelated Gaussian random variables with variance 2NoW. For each E_b/No parameter, the simulation length was 2 million, where the binary bit stream was simulated according to a pseudo-random sequence of length $2^{31}-1$.
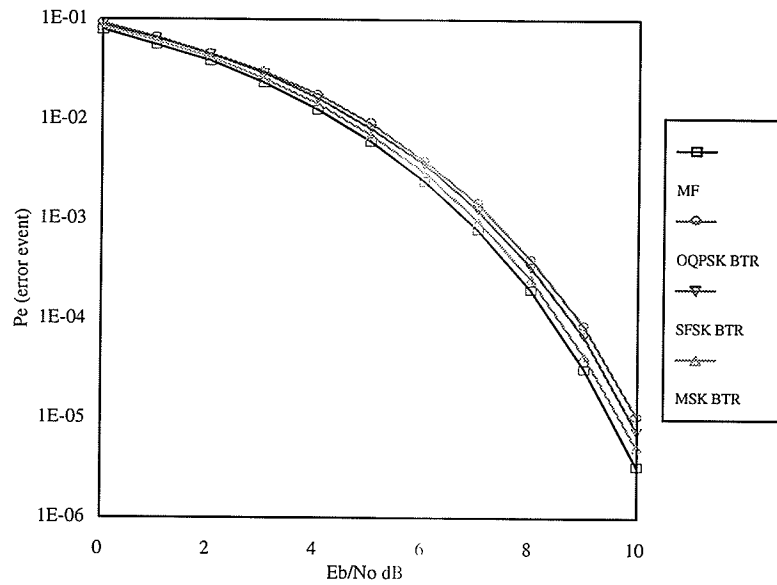
Figure 4-1 BTR performance in AWGN for OQPSK, SFSK and MSK with W=0.5/Tb.
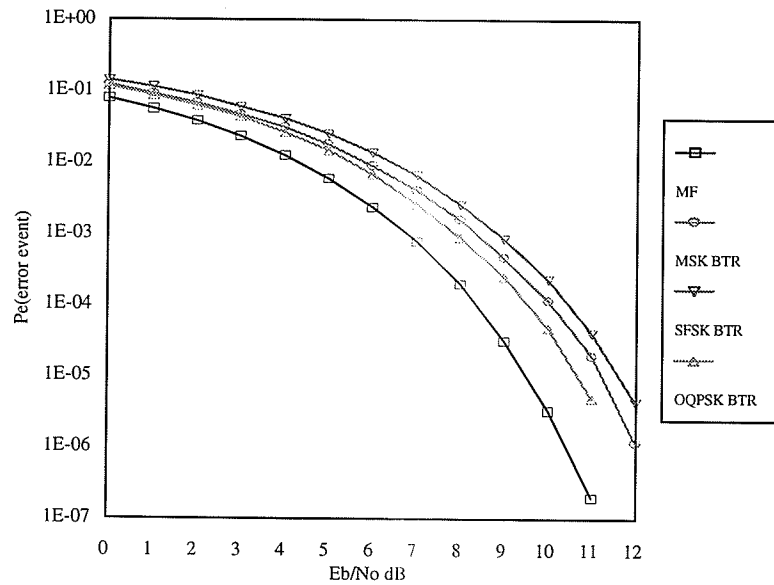
Figure 4-2 BTR performance in AWGN for OQPSK, SFSK and MSK with W=0.25/T$_b$.

The simulation results shown in Figures 4-1, 4-2 with $W=0.5/T_b$ and $W=0.25/T_b$ for OQPSK, MSK, SFSK agree with the d^2_{min} dB loss indicated by the analysis. The performance of these three modulations for the BTR with $W=0.5/T_b$, but particularly the more bandwidth efficient MSK at $W=0.5/T_b$, are practically indistinguishable from the optimum performance of the matched filter.

4.1.3 SR revceiver.

In the case of the filter with $W=0.5/T_b$, sampling the filtered signal at the Nyquist rate introduces at least two serious intersymbol terms. In effect, the trellis decoder is compensating for these ISI terms. A simpler receiver (SR) is one that samples at the symbol rate $(2T_b)$, avoids the two dominant ISI terms, and makes decisions every symbol interval. Ignoring the degradation due to the residual ISI for the symbol rate sampler, the performance of the SR can be lower bounded by the analysis already given. The upper bound on d^2_{min} equals:

$$d^2_{min} \leq \frac{1}{2W}\left\|2g_s\right\|^2 = 4\left[\frac{1}{2W}\left\|g_s\right\|^2\right] \qquad (4.7)$$

where g_s is the peak sample at the output of channel h(t) due to p(t).

The degradation of d^2_{min} compared to the matched filter is given in Table II.

Table II.   SR d^2_{min} loss in dB for $W=0.5/T_b$, and $W=0.25/T_b$

	SR d^2_{min} loss to MF			SR d^2_{min} loss to BTR	
	$W=0.5/T_b$	$W=0.25/T_b$		$W=0.5/T_b$	$W=0.25/T_b$
OQPSK	0.161 dB	1.121 dB		1.153 dB	0.007 dB
MSK	0.534 dB	1.57 dB		0.402 dB	0.01 dB

Table II indicates that the BTR has superior performance to the SR for W=0.5/T_b, but for W=0.25/T_b has indistinguishable performance. The filtered signal of interest is effectively frequency equalized with W=0.25/T_b. The cost , however, is significant d_{min}^2 degradation compared to W=0.5/T_b, which results in poor performance in AWGN and in ACI (shown later).

4.2 BTR PERFORMANCE IN AWGN AND ACI

4.2.1 Error Analysis

There has been error analysis presented for the MF detection of MSK in ACI and AWGN [23]-[24], as well as for the Viterbi detection of continuous phase modulations in ACI and AWGN[25]. Only an outline of these analyses are presented here in order to emphasize the different sensitivity between the MF and the BTR on the statistics of the ACI. The performance of the BTR and MF in ACI and AWGN are then estimated from Monte Carlo simulations, with some results compared with the previous studies to confirm reliability of the simulations.

For discussion, the equivalent baseband received signal r(t) for the inphase branch in AWGN and ACI is:

$$r(t) = As(t) + a(t) + n(t) \qquad (4.8a)$$

$$s(t) = A \sum_j a_j^I p(t - j2T_b) \qquad (4.8b)$$

$$A = \sqrt{2E_b / T_b}$$

$$a(t) = \sum_{i=1}^{Na} \sum_j A_i a_{i,j}^I p_i(t - j2T_b - \lambda_i) \cos(2\pi f d_i t + \theta_i)$$

$$- \sum_{i=1}^{Na} \sum_j A_i a_{i,j}^Q p_i(t - j2T_b - T_b - \lambda_i) \sin(2\pi f d_i t + \theta_i) \qquad (4.8c)$$

45

where Na is the number of interferers, $\{A_i, fd_i, \lambda_i, \theta_i\}$ are the parameters of each interferer, λ_i and θ_i are independent uniform random variables over $(0,2\pi)$, $(-T_b, T_b)$ respectively. It is assumed that all the inphase and quadrature bit streams of the interferers $\{ \mathbf{a^I}, \mathbf{a^Q} \}$ are independent equally likely random variables.

The quadrature correlation filter performs maximum likelihood detection for each quadrature symbol in AWGN. The probability of symbol error, P_e, is the probability that the projection of the received signal, r(t), on the difference signal, $s_2(t)-s_1(t)$, exceeds a certain threshold. Since the signaling in each branch is antipodal the normalized difference signal is just p(t). In the case of AWGN and ACI, then P_e equals:

$$P_e = \int_\alpha f\{\alpha\} Q \left\{ \sqrt{\frac{d_{min}^2 E_b}{2No} + \frac{\alpha}{No}} \right\} d\alpha$$

(4.9)

where $f\{\alpha\}$ is the density of $\alpha = \int_{-T_b}^{T_b} p(t) a(t,\theta_i,\lambda_i,\mathbf{a_i^I},\mathbf{a_i^Q}) dt$ over $i = 1,...,Na$

The important feature of this result is that P_e depends on integrating a Q function which is perturbed by the statistics of the ACI filtered by the MF. Hence P_e is sensitive to the statistics of the match-filtered ACI when the variance of the nuisance parameter, α, is sufficient to degrade performance.

If one now considers the BTR, which performs MLSE on a bandlimited space in AWGN, then the probability of error event P_e for high SNR is now the probability that the projection of the received signal on the minimum bandlimited difference signal exceeds a certain threshold. It has already been verified by computer simulations that the minimum bandlimited difference signal equals:

$$p(t) \otimes h(t+T_b)$$

(4.10)

where $\otimes$ denotes convolution. Recall that the metric operations performed in the sampled domain by the VA are equivalent to the those performed in the Euclidean bandlimited space. Thus the P_e in the case of AWGN and ACI can be formulated as:

$$Pe = \int_{\alpha} f\{\hat{\alpha}\} Q \left\{ \sqrt{\frac{\hat{d}_{min}^2 E_b}{2No} + \frac{\hat{\alpha}}{No}} \right\} d\hat{\alpha} \qquad (4.11)$$

where $f\{\hat{\alpha}\}$ is the density of $\hat{\alpha} = \int_{-15T_b}^{15T_b} \{p(t) \otimes h(t + T_b)\} a(t, \theta_i, \lambda_i, \mathbf{a}_i^I, \mathbf{a}_i^Q) dt$ over $i = 1, ..., Na$

and $\hat{d}_{min}^2$ is the degraded d_{min}^2 due to the bandlimiting filtering. Since the BTR has more random terms of the adjacent signals in the filtered ACI due to the timespan of $h(t)$, the amplitude statistics of the filtered ACI are more Gaussian. The same remarks concerning P_e sensitivity to the statistics of the filtered ACI applies, except that the variance of this filtered ACI should be less because of the additional filtering by the bandlimiting filter $h(t)$.

4.2.2 An example of the statistics of the filtered ACI

For illustration purposes, an estimate of $f\{\alpha\}$ and $f\{\hat{\alpha}\}$ are obtained from Monte Carlo simulations for the case of one adjacent MSK signal frequency offset by $2.0/T_b$ and at 20 dB interference power to signal power ratio (I/S). Comparing the two densities shown in Figures 4-3 and 4-4, $f\{\alpha\}$ is seen as wider spread than $f\{\hat{\alpha}\}$, with a spike around zero which indicates that there is a significant range of synchronization and phase offsets for which the ACI is in fact orthogonal to the SOI. If $f\{\alpha\}$ and $f\{\hat{\alpha}\}$ are both normalized to have the same variance, $f\{\alpha\}$ will be still wider spread than $f\{\hat{\alpha}\}$, and hence these additional 'tails' of the $f\{\alpha\}$ will incur more error at the medium to high SNR range. This illustration serves to suggest that $f\{\alpha\}$ is relatively more detrimental than $f\{\hat{\alpha}\}$ to error performance in the medium to high SNR range.
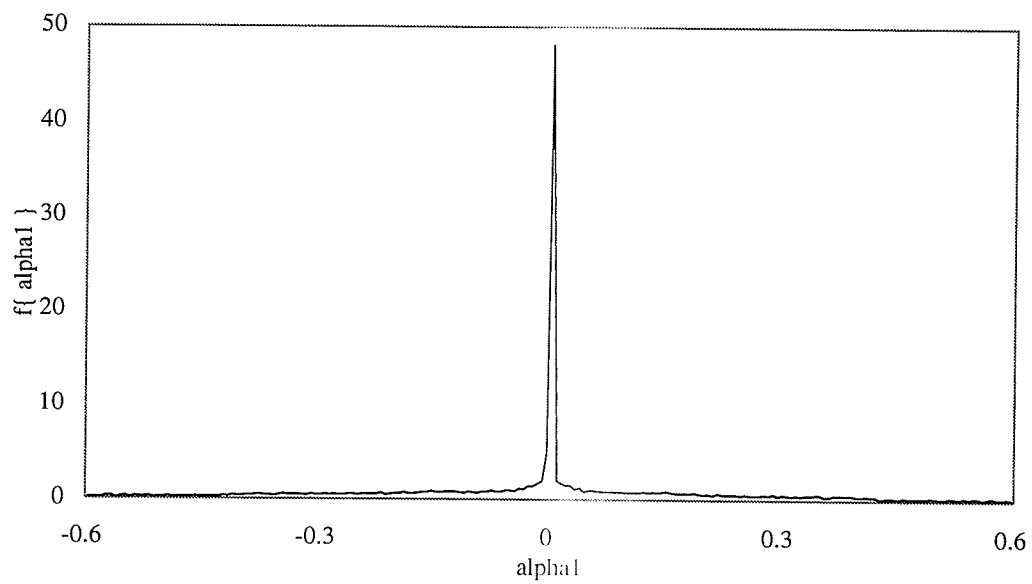
Figure 4-3 Estimate of f{α=alpha1) for adjacent MSK f offset at 2.0/T$_b$ at 20 dB I/S

Figure 4-4 Estimate of f{$\hat{\alpha}$=alpha2) for adjacent MSK offset at 2.0/T$_b$ at 20 dB I/S

4.2.3 Simplified Analysis: Gaussian model

.   A useful analysis to check the performance of the BTR in AWGN and ACI is to model the filtered ACI as AWGN. The probability of error event P_e under this model equals:

$$Pe = Q\left(\sqrt{\frac{\hat{d}_{min}^2 E_b}{2(No + N'o)}}\right) \tag{4.12}$$

where No is the one sided spectral height of the AWGN, $\hat{d}_{min}^2$ is the d_{min}^2 degraded by the filtering and N'o is the equivalent spectral height of the filtered interference in the equivalent baseband model. N'o is computed before the filter by considering one adjacent signal at a frequency offset of f_d , and at an interference to signal ratio of I/S. It is given by:

$$N'o = \frac{(I/S)}{4T_b(2W)} \int_{-W}^{W} \left|P(f - f_d)\right|^2 + \left|P(-f - f_d)\right|^2 df \tag{4.13}$$

4.2.4 Simulation Parameters

Monte Carlo simulations are performed on the BTR and MF receivers in an exact baseband model for the SOI and the ACI, where both the ISI terms of the SOI and the interference terms of the ACI are retained. The simulations are performed under the following parameters:

1)The random parameters { λ, θ_j} are drawn according to their respective density functions every 50 symbol intervals.

2)The run length for each E_b/No simulation run was 2 million, hence providing a reliable estimate of error performance up to 5×10^{-6} (10 errors).

3) The length of each pseudo-random antipodal information sequence is $2^{31}-1$.

The simulations are conducted for MSK and OQPSK for one interferer at f_d equal to $2.0/T_b$, $1,5/T_b$, and $1.0/T_b$. The BTR is simulated for both $W=0.5/T_b$ and $W=0.25/T_b$. One interferer at a relatively high I/S is the most probable near-far situation.

The simulation results are given in terms of average bit error rate for each quadrature branch. Note that errors in each branch in ACI are no longer statistically independent. Thus there may be some benefit in high ACI for the BTR to exploit the correlation between the quadrature branches.

The simulation results are presented as follows. For each frequency spacing f_d, the results for the BTR compared to the analytical results based on modeling the ACI as Gaussian are presented first. Then for each f_d a plot is given. This plot compares the E_b/No dB loss relative to the matched filter at a $P_e=10^{-5}$ in no ACI for each receiver at different levels of I/S. This plot illustrates the relative levels of I/S that each receiver sustains before serious performance degradation.
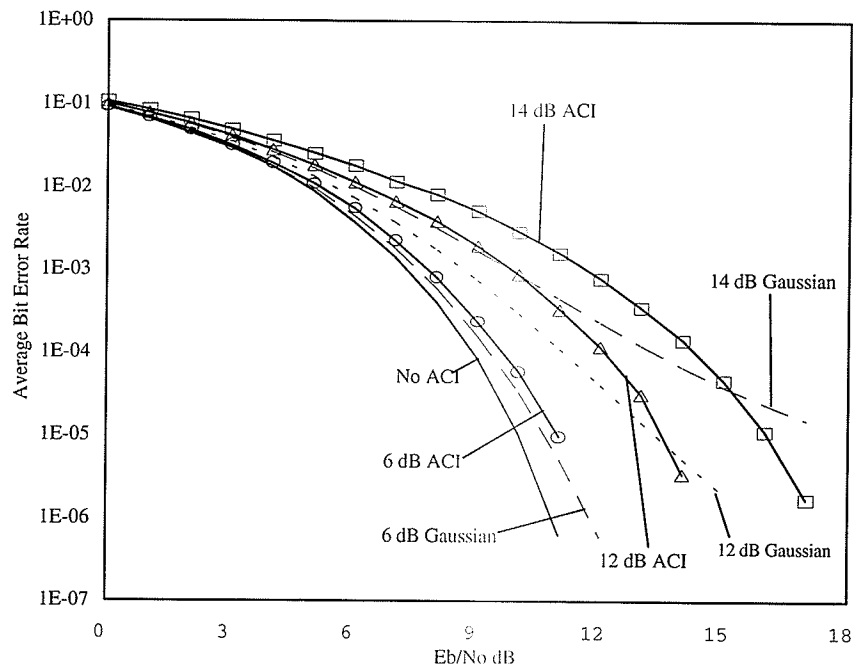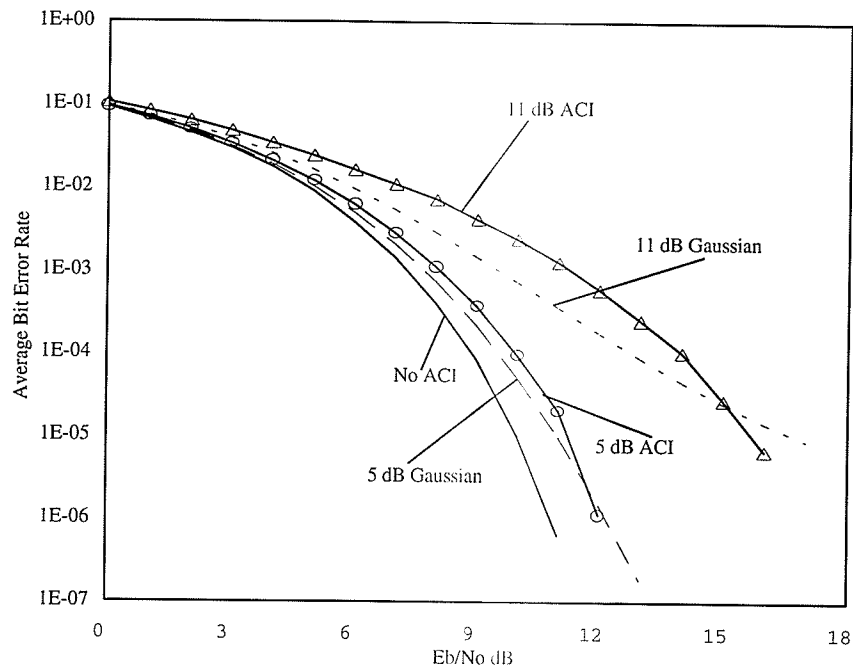
Figure 4-5 OQPSK BTR W=0.5/T$_b$ with one interferer at f$_d$=2.0/T$_b$ and Gaussian model.
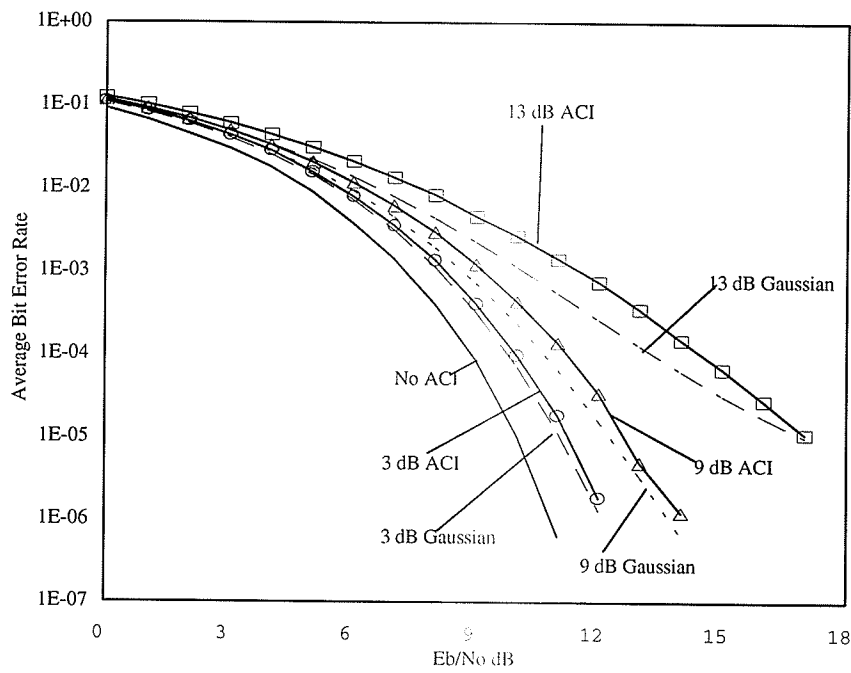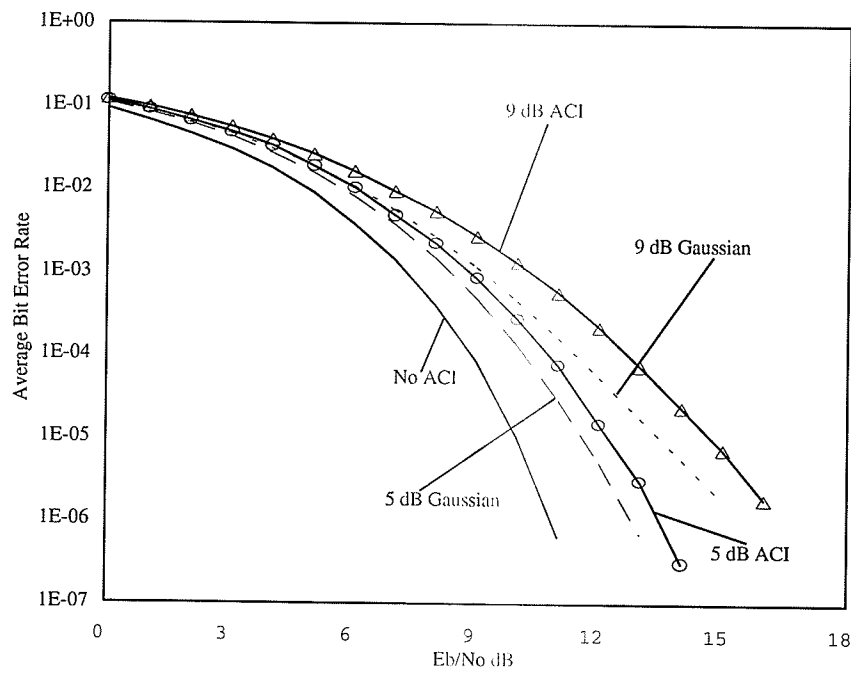

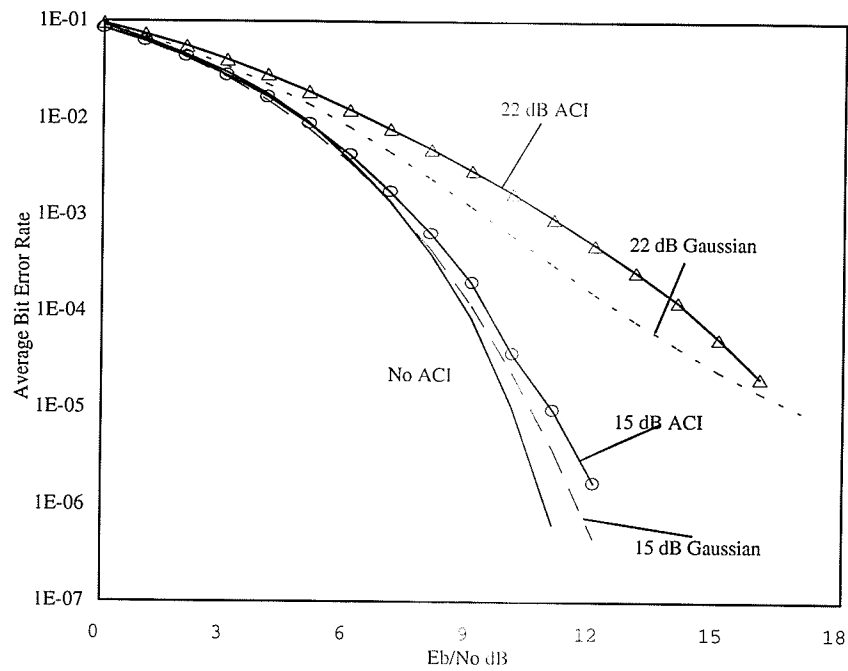**Figure 4-6 OQPSK BTR W=0.25/T$_b$ with one interferer at f$_d$=2.0/T$_b$ and Gaussian Model**
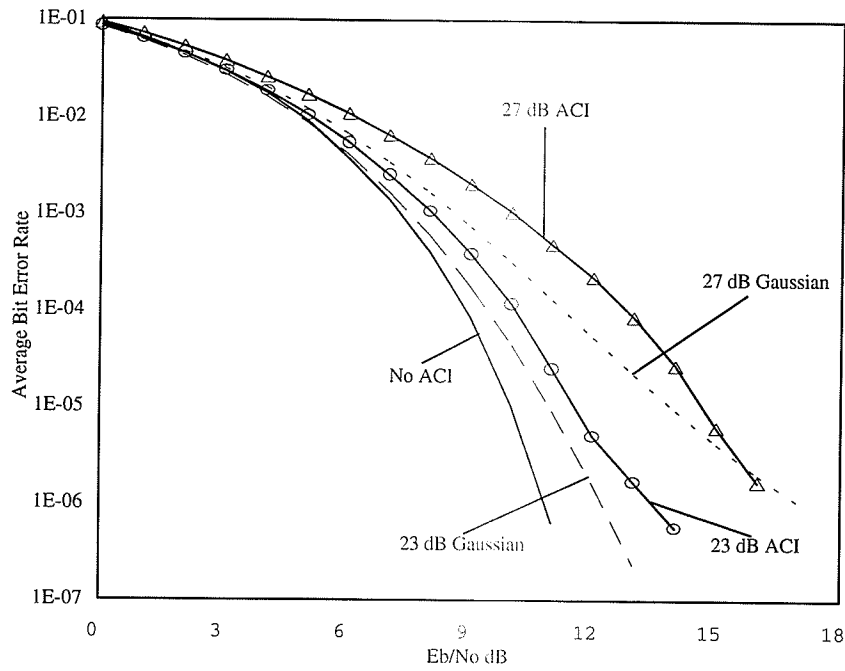
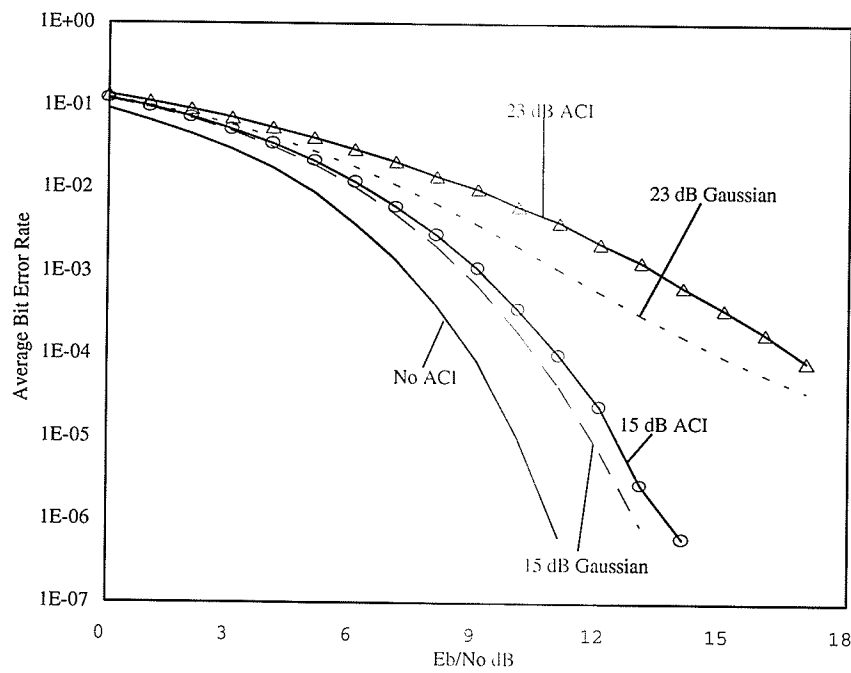**Figure 4-7 MSK BTR W=0.5/T$_b$ with one interferer at f$_d$=2.0/T$_b$ and Gaussian model**
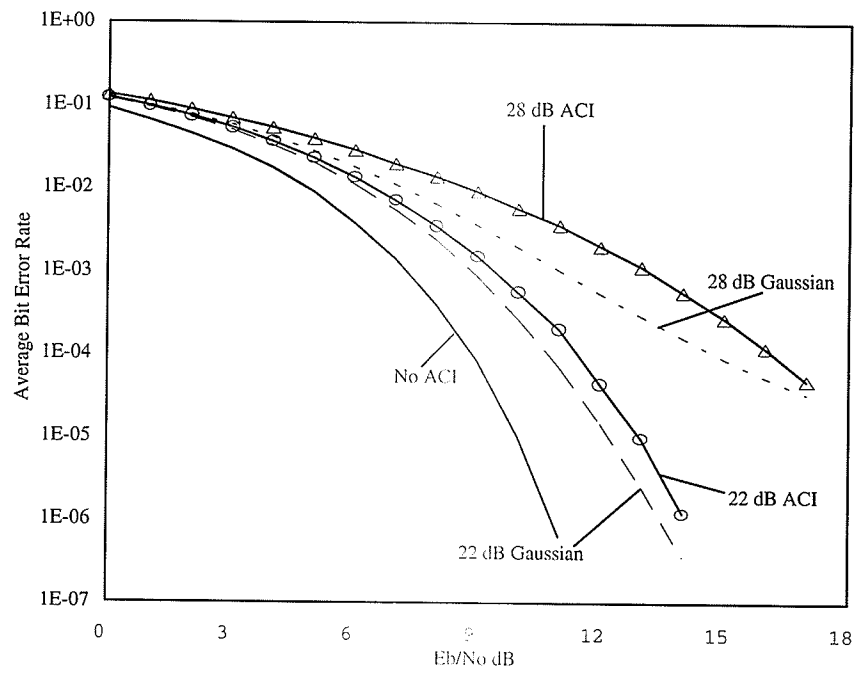
Figure 4-8 MSK BTR W=0.25/T$_b$ with one interferer at f$_d$=2.0/T$_b$ and Gaussian model.
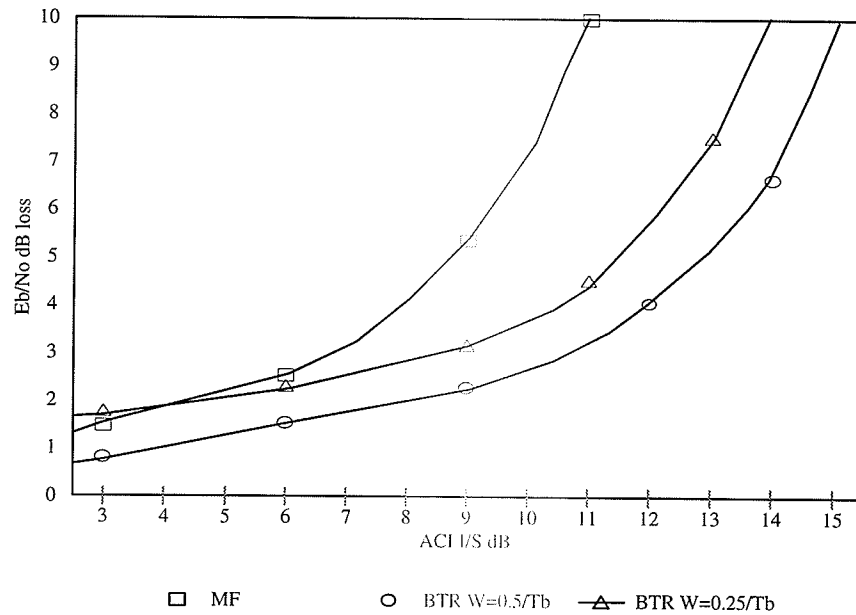
Figure 4-9 E_b/No dB loss compared to MF with no ACI at $P_e=10^{-5}$ for one interferer at $f_d=2.0/T_b$ versus I/S dB for OQPSK
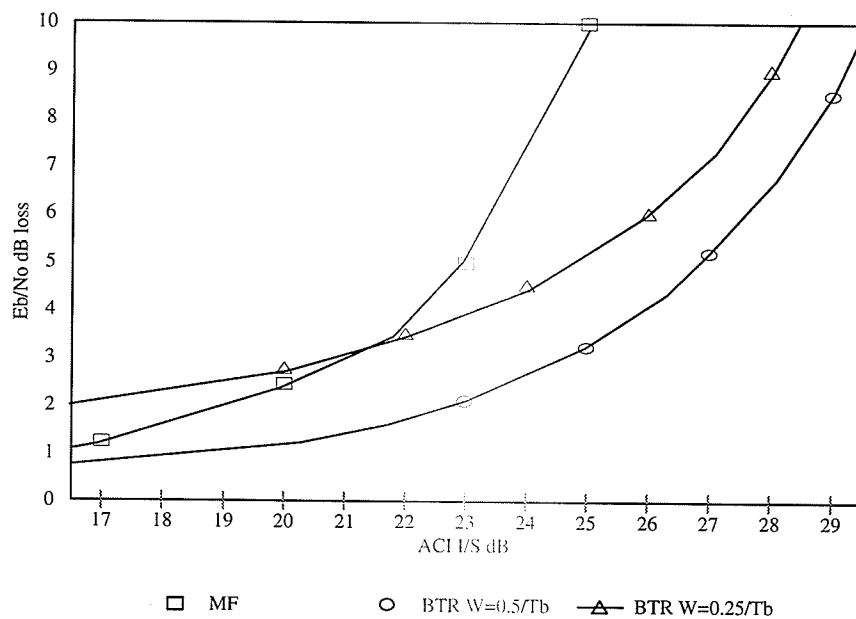
Figure 4-10 E_b/No dB loss compared to MF with no ACI at $P_e=10^{-5}$ for one interferer at $f_d=2.0/T_b$ versus I/S dB for MSK

Figure 4-11 OQPSK BTR W=0.5/T_b with one interferer at f_d=1.5/T_b and Gaussian model.

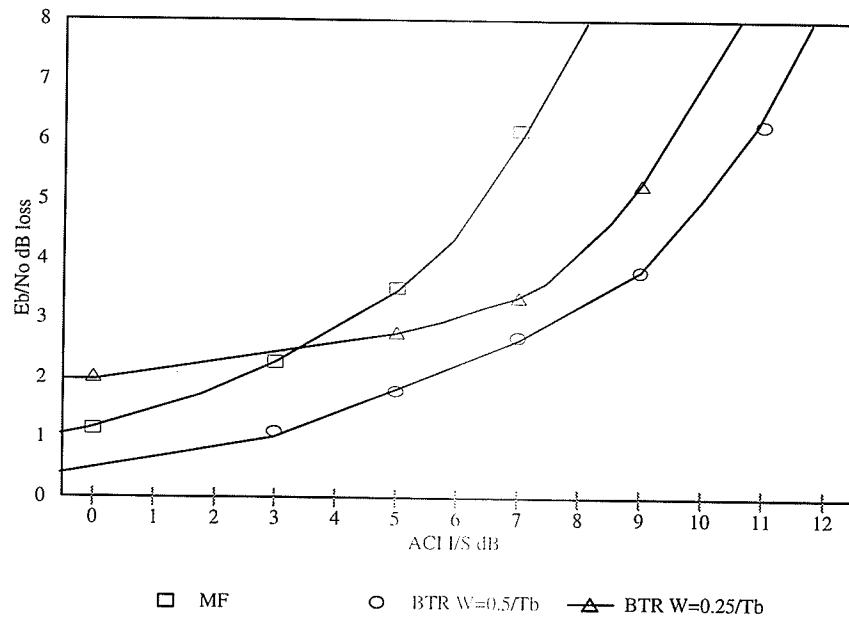**Figure 4-12. OQPSK BTR W=0.25/T_b with one interferer at f_d=1.5/T_b and Gaussian model**

Figure 4-13. MSK BTR W=0.5/T$_b$ with one interferer at f$_d$=1.5/T$_b$ and Gaussian model

Figure 4-14. MSK BTR W=0.25/T$_b$ with one interferer at f$_d$=1.5/T$_b$ and Gaussian model

Figure 4-15. E_b/No dB loss compared to MF with no ACI at $P_e=10^{-5}$ for one interferer at $f_d=1.5/T_b$ versus I/S dB for OQPSK.
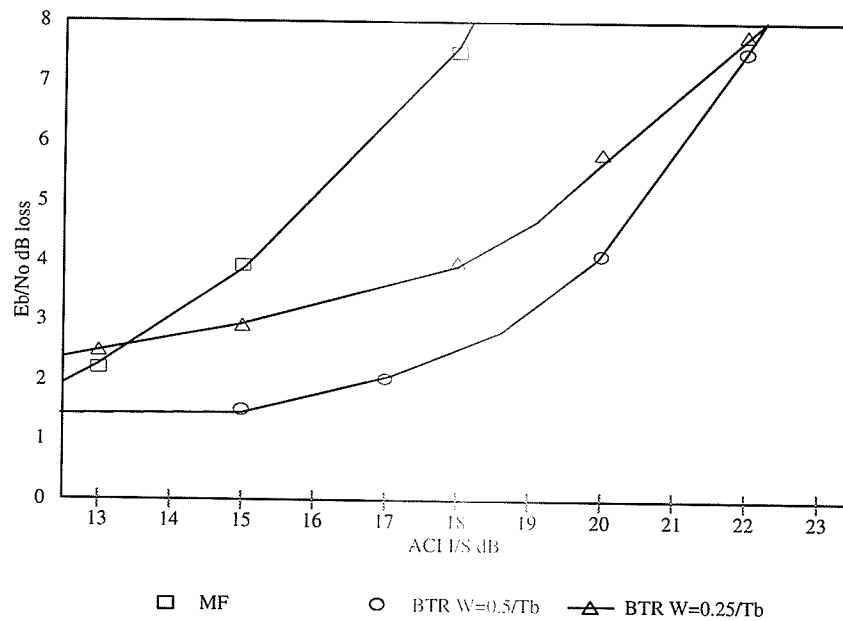

Figure 4-16. E_b/No dB loss compared to MF with no ACI at $P_e=10^{-5}$ for one interferer at $f_d=1.5/T_b$ versus I/S dB for MSK
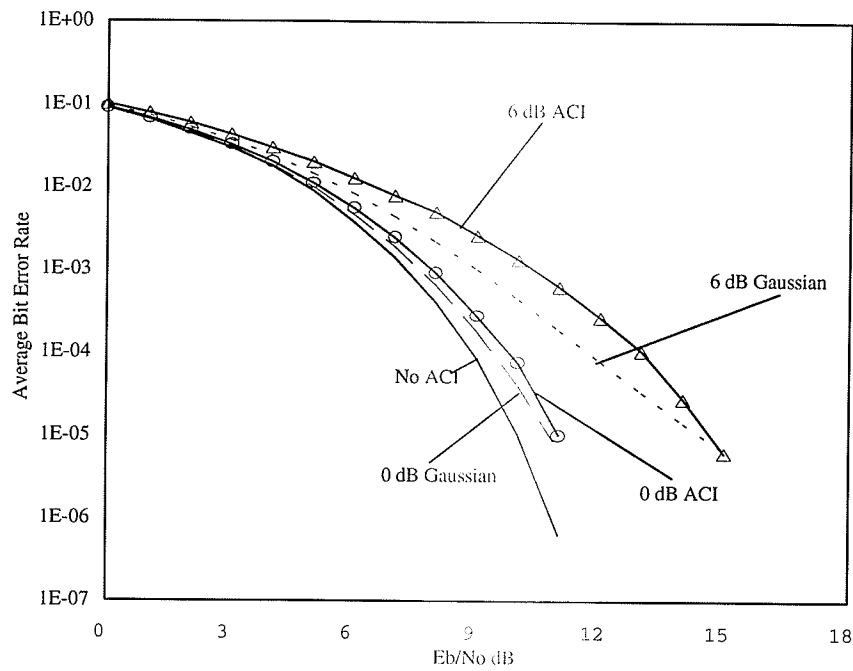
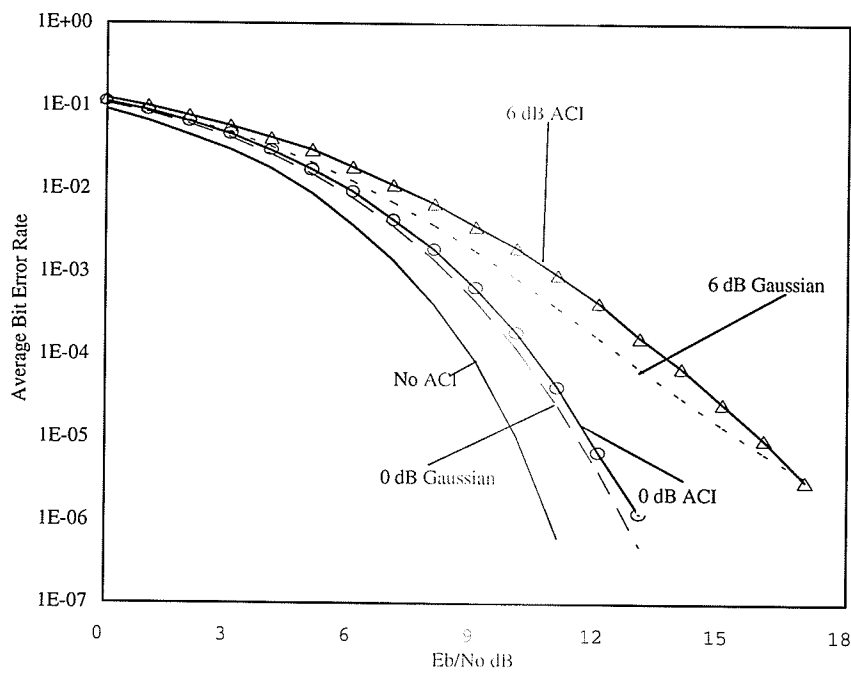**Figure 4-17. OQPSK BTR W=0.5/T_b with one interferer at f_d=1.0/T_b and Gaussian Model**

Figure 4-18 OQPSK BTR W=0.25/T_b with one interferer at f_d=1.0/T_b and Gaussian model
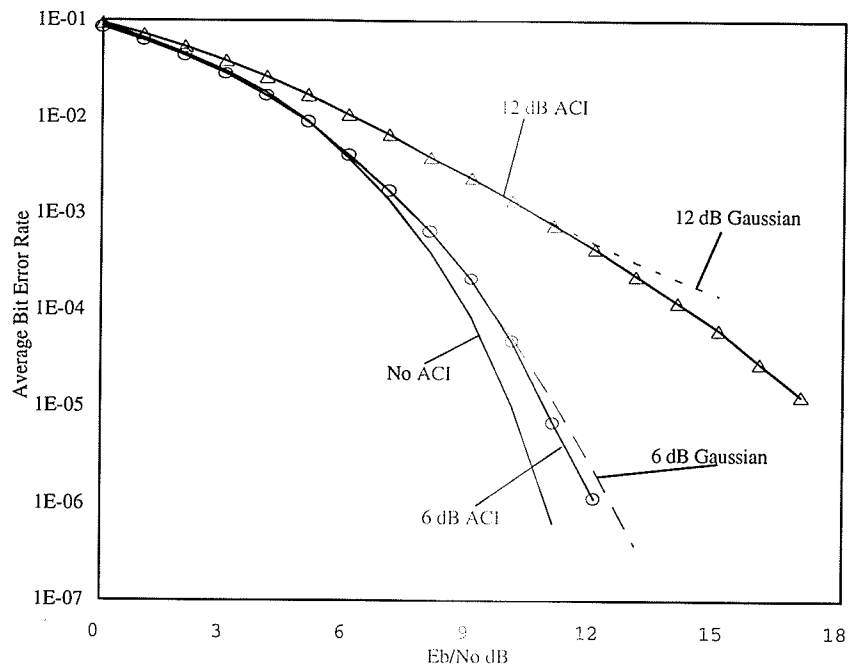
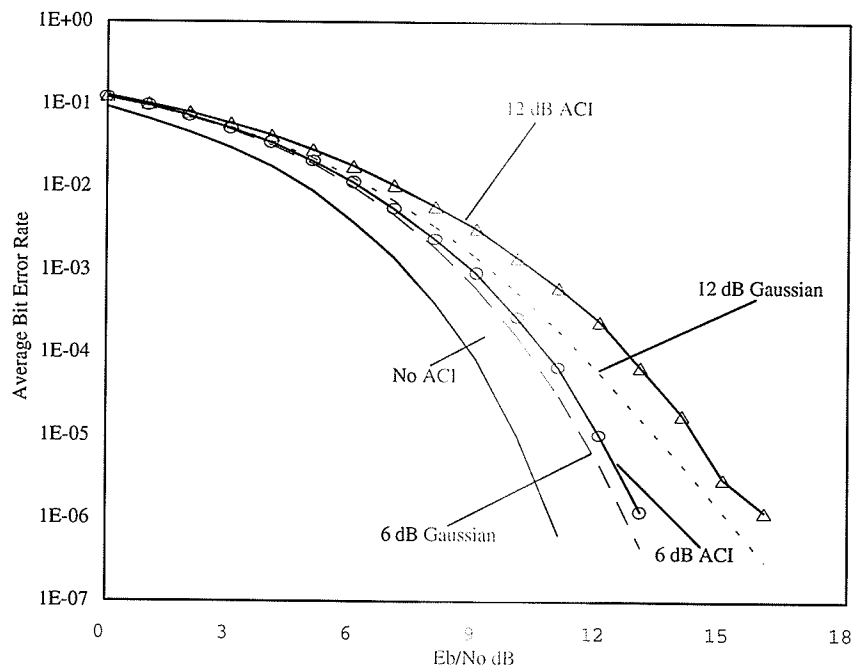**Figure 4-19. MSK BTR W=0.5/T$_b$ with one interferer at f$_d$=1.0/T$_b$ and Gaussian model**

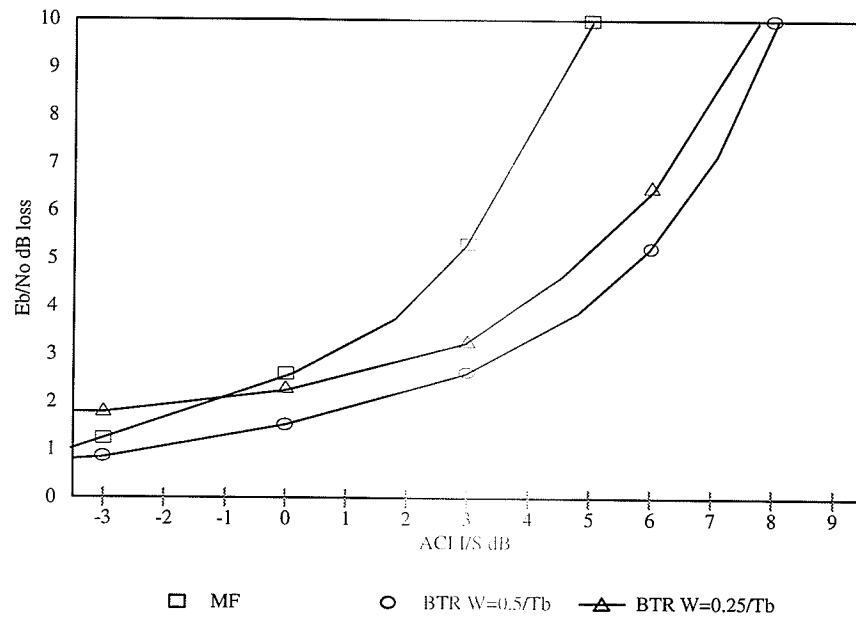**Figure 4-20. MSK BTR W=0.25/T$_b$ with one interferer at f$_d$=1.0/T$_b$ and Gaussian model**

Figure 4-21 E_b/No dB loss compared to MF with no ACI at $P_e=10^{-5}$ for one interferer at $f_d=1.0/T_b$ versus I/S dB for OQPSK
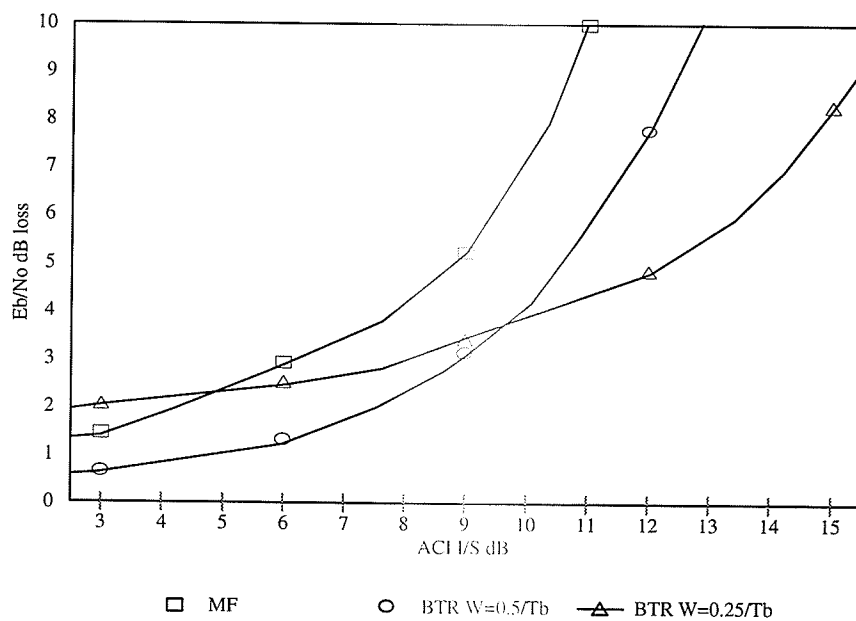

Figure 4-22 E_b/No dB loss compared to MF with no ACI at $P_e=10^{-5}$ for one interferer at $f_d=1.0/T_b$ versus I/S dB for MSK

4.2.5 Simulation Results

In the literature, there is no standard set of parameters or criteria for evaluating ACI. Since there is a whole range of different possible parameters, from frequency spacing to relative power levels between SOI and the ACI, it is difficult to cross reference other results from previous research in this area. For example, the DFE performance in ACI is typically given by the MMSE obtained, not the average bit error performance. One way to compare the two receivers is to approximately determine the threshold of ACI power that each receiver can endure before any serious performance degradation[24]. Typically receivers exhibit a threshold effect under ACI, where when the ACI power is below the threshold there is negligible performance degradation, whereas above this threshold there is rapid degradation. The threshold here is quantified as the Interference to Signal (I/S) power at which the receiver suffers 3 dB loss in performance at an average probability of bit error of 10^{-5}.

The accuracy of the Gaussian model is approximately within 1 dB of the actual performance in ACI for the BTR as shown by Figures 4-5 to 4-22. In general, the Gaussian model gives a slightly over optimistic performance compared to the actual performance in ACI. The differences in performance can be accounted for by the fact the filtered ACI is not white and that there is statistical dependence between the quadrature branches. This approximate agreement between the Gaussian model and the actual performance indicates that modeling the filtered ACI as WGN is a reasonable assumption. There maybe additional benefit in exploring more accurate models for the BTR that

account for the statistical dependence between samples as well as between each quadrature branch.

For the defined threshold of 3 dB Eb/No loss compared to the MF with no ACI at Pe=10^{-5}, Tables III-V give this threshold for MF and BTR as derived from the probability of error plots .

Table III.
I/S dB threshold for OQPSK, and MSK with one interferer at f_d

MF	f_d=1.0/T_b	f_d=1.5/T_b	f_d=2.0/T_b
OQPSK	0.7 dB	4.2 dB	6.8 dB
MSK	6.0 dB	14.0 dB	21.0 dB

Table IV.
I/S dB threshold for the BTR with W=0.5/T_b for OQPSK and MSK with one interferer at f_d and the difference(Δ) in dB to MF for same f_d.

W=0.5/T_b	f_d=1.0/T_b	f_d=1.5/T_b	f_d=2.0/T_b	f_d=1.0/T_b	f_d=1.5/T_b	f_d=2.0/T_b
OQPSK	3.5 dB	7.6 dB	10.5 dB	Δ2.8 dB	Δ3.4 dB	Δ3.7 dB
MSK	8.9 dB	18.8 dB	24.5 dB	Δ2.9 dB	Δ4.8 dB	Δ3.5 dB

Table V.
I/S dB Threshold for the BTR with W=0.25/T_b for OQPSK and MSK with one interferer at f_d and the difference(Δ) in dB to MF for same f_d.

W=0.25/T_b	f_d=1.0/T_b	f_d=1.5/T_b	f_d=2.0/T_b	f_d=1.0/T_b	f_d=1.5/T_b	f_d=2.0/T_b
OQPSK	2.2 dB	5.9 dB	8.5 dB	Δ1.5 dB	Δ1.7 dB	Δ1.7 dB
MSK	8.0 dB	15.1 dB	20.9 dB	Δ2.0 dB	Δ1.1 dB	-Δ0.1 dB

The MF simulation results for MSK at f_d=1.0/T_b and 1.5/T_b, and for OQPSK at f_d=1.0/T_b, agree very closely to the analytical results given in [24]. The BTR with W=0.25/T_b in general performs worse than with W=0.5/T_b. As with the case of AWGN only, the BTR with a narrower bandwidth results in a net performance degradation even though the interference has also been narrowly filtered.

The BTR with $W=0.5/T_b$ for both MSK and OQPSK shows more robustness in suppressing ACI than the MF. The gains in the threshold of above 2.8 dB for these modulations, from the close spacing of $1.0/T_b$ to $2.0/T_b$, compared to the MF can represent significant benefit. The gain of 4.8 dB for MSK at the frequency spacing of $1.5/T_b$ particularly stands out. Of interest is the performance difference of OQPSK and MSK in ACI. The tighter PDS of MSK results in a difference in threshold for the BTR with $W=0.5/T_b$ of 5.4 dB at $f_d=1.0/T_b$ to 14 dB at $f_d=2.0/T_b$. There are clear spectral savings in using MSK compared to OQPSK for either the MF or the BTR.

5. CONCLUSION

The thesis investigated the performance of the BTR in AWGN and ACI for MSK class modulations. Since JMLSE is undesirable because of excess hardware complexity, the receiver in AWGN and ACI must project the received signal onto a subspace. The choice of subspace should have a superior S/I ratio to the matched filter, while having comparable performance to the MF in the case of no interference. A natural choice for unsynchronized FDMA systems is a bandlimited space for the SOI. The BTR performs a MLSE on this bandlimited subspace. The simulation results for the BTR with $W=0.5/T_b$ show that this approach can have comparable performance to the MF in AWGN, with improved performance in ACI from 2.8 dB to 4.8 dB for the cases studied. This approach could be applied to unsynchronized CDMA systems, where one possible subspace could be the same spreading code but with a different pulse shape; one that emphasizes pulse transitions.

The BTR can be applied to bandwidth efficient non-linear modulation such as trellis coded modulation or continuous phase modulation[22]. An appropriate bandlimited space is chosen so as not to degrade the distances in the signal constellation, with the resulting intersymbol interference included in the signal's trellis. For these more bandwidth efficient modulations, such as 64 quadrature amplitude modulation TCM or quaternary partial response CPM, a narrower bandwidth than $0.5/T_b$ may suffice. Note that the resulting ISI from narrowly filtered CPM cannot be frequency equalized in general, since the modulation is non-linear.

Another advantage for the BTR for bandwidth efficient modulations with many states in the trellis is to allow less complex sub-optimum trellis decoding without increased sensitivity to

ACI. Simmons has shown that reduced state decoding of CPM with a matched filter front end is more sensitive to ACI than MLSE decoding of CPM with the VA [22]. The reduced state decoding causes early decisions between two signals before they have merged in the signal trellis. Thus unlike the VA case the difference signal is discontinuous which means that the spectral response of this reduced state decoding receiver rolls off at $1/f^2$. Hence this receiver is highly sensitive to ACI which has the same spectral roll off as OQPSK. The BTR however, already narrowly filters the ACI, which means that early decisions in the signal trellis are subject to less ACI power. In addition, since the filtered ACI is close to Gaussian, the performance of reduced state decoding in ACI for the BTR may be close to the performance in AWGN.

References

1] G.S. Deshpande and P. H. Wittke, "Optimum pulse shaping in digital angle modulation" ,IEEE Trans. Commun.,vol. 29, pp. 162-169, Feb. 1981.

2]B.R. Peterson and D.D. Falconer, "Suppression of Adjacent-Channel, Cochannel, and Intersymbol Interference by Equalizers and Linear Combiners", IEEE Trans. Commun., vol. 42, pp. 3109-3118, Dec. 1994.

3] B.R. Peterson and D.D. Falconer, "Minimum Mean Square Equalization in Cyclostationary and Stationary Interference-Analysis and Subscriber Line Calculations", IEEE Journal on Selected Areas in Communications, Vol. 9, pp 931-940, August 1991.

4]Harry L. Van Trees. Detection, Estimation, and Modualtion Theory- PART 1. John Wiley & Sons, 1968. pp. 246-287

5] Harry L. Van Trees. Detection, Estimation, and Modualtion Theory- PART 1. John Wiley & Sons, 1968. pp. 333-366

6]Gerhard Kramer in conversation in 1994.

7]Sergio Verdu, "Minimum Probability of Error for Asynchronous Gaussian Multiple-Access Channels", IEEE Trans. on Information Theory, VOL. IT-32, pp. 85-96, Jan. 1986.

8]K. Giridhar, S. Chari, J. J. Shynk, and R. P. Gooch, "Joint demodulation of cochannel signals using MLSE and MAPSD algorithms" , in Proc. IEEE Int. Conf. on Acoustics, Speech, and Signal Processing, pp. 640-655, April 1993.

9]R.Y. Hongui and I. Kalet, "MSK-Type Signals in the Presence of Adjacent Channel Interference and White Noise", to be published.

10]R.E. Eaves and S.M. Wheatley, "Optimization of Quadrature-Carrier Modulation for Low Crosstalk and Close Packing of Users", IEEE Trans. Commun, VOL. COM-27, pp. 176-185., Jan. 1979.

11]Irving Kalet, "A Look at Crosstalk in Quadrature-Carrier Modulation Systems", IEEE Trans. Commun, VOL. COM-25, pp. 884-892., Sept. 1977.

12]M. Abdulrahman and D.D Falconer, "Cyclostationary Crosstalk Suppression by Decision Feedback Equalization on Digital Subscriber Loops", IEEE Journal on Selected Areas in Communications, VOL. 10, pp. 640 -648.

13]P. Niger and P. Vandamme, "Performance of Equalization Techniques in a Radio Interference Environment" , IEEE Trans. Commun. , VOL. 39, pp. 452-458, March 1991.

14]W. A. Gardner, "Cyclic Wiener Filtering: Theory and Method", IEEE Trans. Commun., VOL. 41, pp. 151-163, Jan. 1993.

15]W.A. Gardner, W. A. Brown III, and C.K. Chen, "Spectral Correlation of Modulated Signals: Part II- Digital Modulation", IEEE Trans. Commun.,VOL. COM-35, pp.595-601, June 1987.

16]M. Abdulrahman, A.U.H. Sheikh, and D.D. Falconer, "Decision Feedback Equalization for CDMA in Indoor Wireless Communications" , IEEE Journal on Selected Areas in Comm. , VOL. 12, pp. 698 - 705., May 1994.

17]John Proakis. Digital Communications. Second Edition. Mcgraw-Hill. 1989. p. 600.

18]G. D. Forney , "Maximum-Likelihood Sequence Estimation of Digital Sequences in the Presence of Intersymbol Interference ", Trans. on Information Theory, VOL. IT-18, pp.363-377, May 1972.

19] G. Ungerboeck, "Adaptive Maximum-Likelihood Receiver for Carrier-Modulated Data - Transmission Systems ", IEEE Trans. Commun., VOL. COM-22, pp. 624-636, May 1974

20]S.J Simmons, "Simplified Coherent Detection of Bandwidth-Efficient CPFSK/CPM Modulations", IEEE Pac.Rim. Conf. on CCSP, Victoria, B.C., May 1991, pp. 174-177.

21]S.J. Simmons, "ACI Susceptibility of Reduced-State Decoding for CPM, Biennial Sumposium on Communications -Queen's University, pp. 261-264, 1992.

22]S.J Simmons, "Simplified Coherent Detection of CPM" , IEEE Trans. Commun., VOL. 43, pp. 726-728, Feb/March/April 1995.

23]J. R. Cruz, R. S. Simpson, "Cochannel and Intersymbol Interference in Quadrature-Carrier Modulation Systems", IEEE Trans. Commun., VOL. 29, pp 285-297, March 1981.

24]R.B. Rhodes Jr, S. G. Wilson, and N.A.B. Svensson, "MSK-Type Reception of Continuous Phase Modulation: Cochannel and Adjacent Channel Interference", IEEE Trans. Commun., VOL. COM-35, pp. 185-193, Feb. 1987.

25]N.A.B. Svensson, "Error Probability Analysis for Continuous Phase Modulation with Viterbi Detection on a Gaussian Channel with Multiple Signal Interference" , IEEE Trans. Commun., VOL. 37, pp. 230-237, March 1989.